

AD-A101 497

AIR FORCE INST OF TECH WRIGHT-PATTERSON AFB OH
MAXIMUM INFORMATION TRAJECTORY FOR AN AIR-TO-AIR MISSILE INTERC--ETC(U)
DEC 80 S W LARSON
AFIT-CI-80-68T

F/6 16/2

UNCLASSIFIED

NL

for
AC
ADP 497

END
DATE
FILED
8-88
DTIC

(14)

UNCLASS

(1)

SECURITY CLASSIFICATION OF THIS PAGE (When Data Entered)

AFIT

- CI - REPORT DOCUMENTATION PAGE

READ INSTRUCTIONS
BEFORE COMPLETING FORM

ADA101497

1. REPORT NUMBER 80-68T	2. GOVT ACCESSION NO. AD-A101 499	3. RECIPIENT'S CATALOG NUMBER
4. TITLE (and Subtitle) Maximum Information Trajectory For An Air-to-Air Missile Intercept		5. TYPE OF REPORT & PERIOD COVERED THESIS/DISSERTATION
6. AUTHOR Capt Stephen Wendell Larson	7. PERFORMING ORG. REPORT NUMBER WPAFB OH 45433	
8. CONTRACT OR GRANT NUMBER(S)		9. PERFORMING ORGANIZATION NAME AND ADDRESS AFIT STUDENT AT: Univ of Texas at Austin
10. PROGRAM ELEMENT, PROJECT, TASK AREA & WORK UNIT NUMBERS		11. CONTROLLING OFFICE NAME AND ADDRESS AFIT/NR WPAFB OH 45433
12. REPORT DATE Dec 80		13. NUMBER OF PAGES 78
14. MONITORING AGENCY NAME & ADDRESS (if different from Controlling Office) L-721		15. SECURITY CLASS. (of this report) UNCLASS
16. DISTRIBUTION STATEMENT (of this Report) APPROVED FOR PUBLIC RELEASE; DISTRIBUTION UNLIMITED		17. DISTRIBUTION STATEMENT (of the abstract entered in Block 20, if different from Report) S DTIC ELECTE JUL 17 1981 D
18. SUPPLEMENTARY NOTES APPROVED FOR PUBLIC RELEASE: IAW AFR 190-17 23 JUN 1981		
19. KEY WORDS (Continue on reverse side if necessary and identify by block number)		
20. ABSTRACT (Continue on reverse side if necessary and identify by block number) ATTACHED		

81 7 16 024

AFIT RESEARCH ASSESSMENT

80-68T

The purpose of this questionnaire is to ascertain the value and/or contribution of research accomplished by students or faculty of the Air Force Institute of Technology (ATC). It would be greatly appreciated if you would complete the following questionnaire and return it to:

AFIT/NR
Wright-Patterson AFB OH 45433

RESEARCH TITLE: Maximum Information Trajectory for an Air-to-Air Missile Intercept

AUTHOR: Stephen Wendell Larson

RESEARCH ASSESSMENT QUESTIONS:

NAME _____ GRADE _____ POSITION _____

ORGANIZATION _____ LOCATION _____

STATEMENT(s):

Accessories for
MEIS GRANT
DTIC TAB
Unannounced
Justification

Per
Distribution/
Availability Codes
Avail and/or
Dist Special

A

FOLD DOWN ON OUTSIDE - SEAL WITH TAPE

AFIT/NR
WRIGHT-PATTERSON AFB OH 45433

OFFICIAL BUSINESS
PENALTY FOR PRIVATE USE. \$300



NO POSTAGE
NECESSARY
IF MAILED
IN THE
UNITED STATES

BUSINESS REPLY MAIL
FIRST CLASS PERMIT NO. 73236 WASHINGTON D.C.

POSTAGE WILL BE PAID BY ADDRESSEE

AFIT/ DAA
Wright-Patterson AFB OH 45433



FOLD IN

MAXIMUM INFORMATION TRAJECTORY FOR AN
AIR-TO-AIR MISSILE INTERCEPT

APPROVED:

David B. Hull
Jason D. Speyer

MAXIMUM INFORMATION TRAJECTORY FOR AN
AIR-TO-AIR MISSILE INTERCEPT

BY

STEPHEN WENDELL LARSON, B.S.A.E.

THESIS

Presented to the Faculty of the Graduate School of
The University of Texas at Austin
in Partial Fulfillment
of the Requirements
for the Degree of

MASTER OF SCIENCE IN ENGINEERING

THE UNIVERSITY OF TEXAS AT AUSTIN

December, 1980

ABSTRACT

This thesis presents a method for finding the trajectory to complete an air-to-air missile intercept which maximizes information. This is accomplished by formulating a parameter optimization problem and using a penalty function-Lagrange multiplier method to solve for the optimal path. The performance index is the trace of the information matrix. This information matrix is derived using an extended Kalman filter formulation, in cartesian coordinates, which makes state estimates based only on angle measurements. The trace operation on the information matrix is used because the trace and the integration operations commute allowing a scalar performance index. Further, reduction in the functional form of the performance index is achieved by weighing the information matrix by the inverse of the measurement power spectral density. This also avoids numerical difficulties near intercept.

TABLE OF CONTENTS

Abstract	iv
List of Tables	vii
List of Figures	viii
Nomenclature	x
I. INTRODUCTION	1
II. GEOMETRY	4
2.1 Inertial Axis System	4
2.2 Missile Axis Systems	4
2.3 Target System	9
2.4 Launch Geometry	9
III. MODELS	13
3.1 Missile Model	13
3.2 Target Model	21
3.3 Atmospheric Model	21
IV. THE INFORMATION INDEX	22
4.1 Definition	22
4.2 The Dynamical System	24
4.3 The State Transition Matrix	28
4.4 Angle Measurement Noise	30
4.5 The Weighting Matrix	31

4.6	The Performance Index	32
V.	PROBLEM FORMULATION	34
5.1	The Optimal Control Problem	34
5.2	The Parameter Optimization Method	38
VI.	SOLUTION METHOD	41
6.1	Input	41
6.2	Optimization Method	41
6.3	Function Evaluation	44
6.4	Numerical Derivatives	45
6.5	Optimization Algorithm	46
VII.	RESULTS	47
7.1	Launch Scenarios	47
7.2	Results and Conclusions	48

LIST OF TABLES

1.	Aerodynamic Coefficients, Functions of M	16
2.	Aerodynamic Coefficients, $C_N(\alpha, M)$	17
3.	Intercept Results	50

LIST OF FIGURES

1. Missile Axes Systems	7
2. Launch Geometry	10
3. Intercept Geometry and Measurement Angles	11
4. Lift and Drag	18
5. Boresight Angle	18
6. Function Evaluation	44
7. Best Information Horizontal Trajectory, 3000', 0°	52
8. Best Information Vertical Trajectory, 3000', 0°	52
9. Best Information Boresight Angle, 3000', 0°	53
10. Best Information Boresight Angle Rate, 3000', 0°	53
11. Best Information Az and El Angles, 3000', 0°	54
12. Best Information Az and El Angle Rates, 3000', 0°	54
13. Best Information Horizontal Trajectory, 3000', 30°	55
14. Best Information Vertical Trajectory, 3000', 30°	55
15. Best Information Boresight Angle, 3000', 30°	56
16. Best Information Boresight Angle Rate, 3000', 30°	56
17. Best Information Az and El Angles, 3000', 30°	57
18. Best Information Az and El Angle Rates, 3000', 30°	57
19. Best Information Horizontal Trajectory, 7000', 60°	58
20. Best Information Vertical Trajectory, 7000', 60°	58
21. Best Information Boresight Angle, 7000', 60°	59

22.	Best Information Boresight Angle Rate, 7000', 60°	59
23.	Best Information Az and El Angles, 7000', 60°	60
24.	Best Information Az and El Angle Rates, 7000', 60°	60
25.	Minimum Time Horizontal Trajectory	61
26.	Minimum Time Vertical Trajectory	61
27.	Minimum Time Boresight Angle	62
28.	Minimum Time Boresight Angle Rate	62
29.	Minimum Time Az and El Angles	63
30.	Minimum Time Az and El Angle Rates	63

NOMENCLATURE

a	control parameter vector
$a_{T_X}, a_{T_Y}, a_{T_Z}$	target inertial acceleration components (ft/sec^2)
az, el	azimuth and elevation measurement angles (deg)
a_{Z_B}	missile normal acceleration (g 's)
a_1, a_2, b_1, b_2	measurement noise constants
b	parameter vector
g	acceleration of gravity (ft/sec^2)
	time-normalized equations of motion
	observation-state relation
h	altitude above sea level (ft)
i_B, j_B, k_B	unit vectors along missile body axes
i_I, j_I, k_I	unit vectors along inertial axes
i_W, j_W, k_W	unit vectors along missile wind axes
k	number of equality constraints
m	number of constraints
	mass (slugs)
n	number of control parameters
t	time (sec)
tr	trace operator
u	control vector
x	state vector for missile model

z	measurement vector
AAY	launch yaw aspect angle (deg)
BAY	launch boresight angle (deg)
C	constraint residuals
C_{a_0}	axial force coefficient for $\alpha = 0$
$C_{D\alpha}$	drag coefficient due to angle of attack
$C_{D\alpha^2}$	drag coefficient due to angle of attack squared
$C_{N\alpha}$	normal force coefficient due to angle of attack
C_{N_0T}	intercept in C_N interpolation
D	drag (1b)
F	characteristic matrix for state vector
F_X, F_Z	missile body axis forces (1b)
G	characteristic matrix for the control vector
GC	matrix of first derivatives of C with respect to b
$G\phi$	matrix of first derivatives of ϕ with respect to b
H	matrix of first derivatives of g with respect to X
HH	intermediate values in the performance index
I	information matrix
J	performance index
L	lift (1b)
M	Mach number
P	error covariance matrix
	penalty function

R_{az}, R_{el}	azimuth and elevation measurement ranges
S	missile reference area (ft^2)
	optimization weighting matrix
T	missile thrust
T_1	inertial to wind axis transformation matrix
T_2	wind to body axis transformation matrix
U_R, V_R, W_R	inertial relative velocity components (ft/sec)
V	matrix of measurement noise power spectral densities
V_M	missile velocity (ft/sec)
$V_{T_X}, V_{T_Y}, V_{T_Z}$	target inertial velocity components (ft/sec)
W	missile weight (lb)
	weighting matrix
X	state vector for dynamical system
X_B, Y_B, Z_B	missile body axes
X_I, Y_I, Z_I	inertial axis coordinates (ft)
X_M, Y_M, Z_M	missile inertial position components (ft)
X_R, Y_R, Z_R	missile/target relative position coordinates (ft)
X_T, Y_T, Z_T	target inertial position components (ft)
X_W, Y_W, Z_W	missile wind axes
α	missile angle of attack (deg)
β	optimization factors
Γ	optimization factors
Δx	perturbation of x

ϵ small number
 θ inequality constraint residuals
 λ target acceleration constant (sec^{-1})
 ρ atmospheric density (slug/ft^3)
 σ elements of weighting matrix
 τ dummy variable of integration
normalized time component
 ϕ performance index as a function of b
 Φ state transition matrix
 X, Y, μ missile wind axis yaw, pitch and roll angles (deg)
 ψ, θ missile body axis yaw and pitch angles (deg)
 Ψ equality constraint residuals
 Ω boresight angle (deg)

subscripts

0 condition at $t=0$
 f condition at final time
 x partial with respect to x
 M missile
 T target

superscripts

$.$ derivative with respect to time
 -1 inverse
 T transpose

SECTION I
INTRODUCTION

Many of the modern, tactical, air-to-air missiles employ passive seekers such as infrared heat seekers in their guidance systems. For particular geometries where the line-of-sight inertial angle is small, the proportional navigation system, which drives the inertial line-of-sight angle rate to null, works reasonably well. If the intercept geometry is more severe, or if the target is accelerating, then obtaining range and range-rate information becomes important, especially to derive the time-to-go to intercept. Since passive or jammed sensors may only have angle information, range and range rate can only be obtained by extraction from sophisticated filter design.

In Reference 1, Sammons et al compare various implementations of the extended Kalman filter for missile onboard operations. This filter uses angle measurements to estimate relative position, relative velocity, and target acceleration. Estimates of range and range rate are physically obtained by having the inertial line-of-sight angle constantly changing. However, the proportional navigation guidance law is always attempting to drive the angle rate to zero. Since these angles are the only source of information, it seems obvious that, when the angle rate approaches zero, there will be little or no information to the filter about range and range rate. The guidance law is working

against the estimator by commanding a flight path which denies information to the estimator.

The purpose of this thesis is to find and investigate the optimal trajectory which completes a missile intercept such that some measure of information is maximized. In this way the filter can make the most accurate state estimate possible. It is not suggested here that this be the only measure of performance, but that it be an element in developing a composite performance criteria.

The particular missile under consideration is a highly-maneuverable, short-range, bank-to-turn, air-to-air missile capable of 100 normal g's. The missile model, that is, the aerodynamics, the autopilot, the guidance law, etc., is completely developed in Reference 2. The geometry of the intercept and the missile model are discussed in Sections II and III.

The measure of information chosen is the information matrix. Measures on the information matrix imply the relative observability in estimating the state due to measurement functions alone. This means that the relative observability of the system is obtained only from the deterministic system model of the dynamics and measurement. The information matrix and its use as a performance index is developed in Section IV.

In Section V, the optimal control problem is formulated. The parameter optimization method is then discussed, and all the constraints are derived.

The optimization method used to solve this problem is the penalty function - Lagrange multiplier method discussed by Fletcher in

Reference 3. This is a state-of-the-art method for solving parameter optimization problems. It is particularly convenient since it requires very little set up time and can be used with equality constraints and inequality constraints at the same time. Section VI contains a brief discussion of this method along with discussions of the function evaluations and numerical derivatives.

Finally, the results are presented in Section VII. The various launch scenarios are described, and some concluding remarks are presented.

SECTION II

GEOMETRY

This section covers the problem set-up. The various reference systems and their relationships are discussed, and the launch and intercept geometries are described.

2.1 Inertial Axis System.

The inertial axis system is a standard right-handed system with the positive Z_I axis pointing toward the center of the earth. The origin is at mean sea level with the missile launch point lying on the negative Z_I axis. Because of this, the magnitude of the Z_I component of the respective position vector corresponds to the altitude of the missile or target.

2.2 Missile Axis Systems.

There are two axis systems associated with the missile - a wind axis and a body axis system. These two systems share a common origin, assumed to be at the missile center of gravity.

The wind axis system is a standard right-handed system with the X_W axis tangent to the flight path and positive forward. The Z_W axis is perpendicular to the X_W axis, in the plane of symmetry, and positive down if the missile is in normal, level flight. The Y_W axis is situated perpendicular to the X_W - Z_W plane to complete the right-hand system. The angular relationship with the inertial system is through

the velocity yaw angle, χ , the velocity pitch angle, γ , and the velocity roll angle, μ . This angular relationship is derived in Reference 4 and given by

$$\begin{bmatrix} i_w \\ j_w \\ k_w \end{bmatrix} = \begin{bmatrix} \cos\gamma\cos\chi & \cos\gamma\sin\chi & -\sin\gamma \\ \sin\mu\sin\gamma\cos\chi & \sin\mu\sin\gamma\sin\chi & \sin\mu\cos\gamma \\ -\cos\mu\sin\chi & +\cos\mu\cos\chi & \\ \cos\mu\sin\gamma\cos\chi & \cos\mu\sin\gamma\sin\chi & \cos\mu\cos\gamma \\ +\sin\mu\sin\chi & -\sin\mu\cos\chi & \end{bmatrix} \begin{bmatrix} i_I \\ j_I \\ k_I \end{bmatrix} \quad (1)$$

The missile body axis system is described by the positive X_B axis directed through the nose of the missile. The Z_B axis is perpendicular to the X_B axis, in the plane of symmetry, and positive down if the missile is in normal, level flight. The Y_B axis is situated to complete the right-hand system. It is assumed that there is no side-slip angle; therefore, the body axes and the wind axes are related only through the angle of attack, α . This relationship is also derived in Reference 4 and is given by

$$\begin{bmatrix} i_B \\ j_B \\ k_B \end{bmatrix} = \begin{bmatrix} \cos\alpha & 0 & -\sin\alpha \\ 0 & 1 & 0 \\ \sin\alpha & 0 & \cos\alpha \end{bmatrix} \begin{bmatrix} i_w \\ j_w \\ k_w \end{bmatrix} \quad (2)$$

The missile body axis system is related to the inertial system through the body yaw angle ψ , and the body pitch angle θ . These two angles completely define the orientation of the body longitudinal axis in inertial space, and are used as the control variables in the optimal control problem. The inertial to body angular relationship is derived by successive rotations about the yaw axis and the pitch axis and is given by

$$\begin{bmatrix} i_B \\ j_B \\ k_B \end{bmatrix} = \begin{bmatrix} \cos\theta\cos\psi & \cos\theta\sin\psi & -\sin\theta \\ -\sin\psi & \cos\psi & 0 \\ \sin\theta\cos\psi & \sin\theta\sin\psi & \cos\theta \end{bmatrix} \begin{bmatrix} i_I \\ j_I \\ k_I \end{bmatrix} . \quad (3)$$

The relationship of the missile axis system to the inertial axis system is shown in Figure 1.

The angles α and μ can be found from the angles ψ , θ , χ , and γ . ψ and θ are the control angles, and, therefore, known; χ and γ are part of the state vector, and, therefore, also known. The solution is found by transforming from the inertial system through the wind axes to the body axes. If Equations (1) and (2) are rewritten as

$$\begin{bmatrix} i_W \\ j_W \\ k_W \end{bmatrix} = T_1 \begin{bmatrix} i_I \\ j_I \\ k_I \end{bmatrix} \quad \begin{bmatrix} i_B \\ j_B \\ k_B \end{bmatrix} = T_2 \begin{bmatrix} i_W \\ j_W \\ k_W \end{bmatrix} , \quad (4)$$

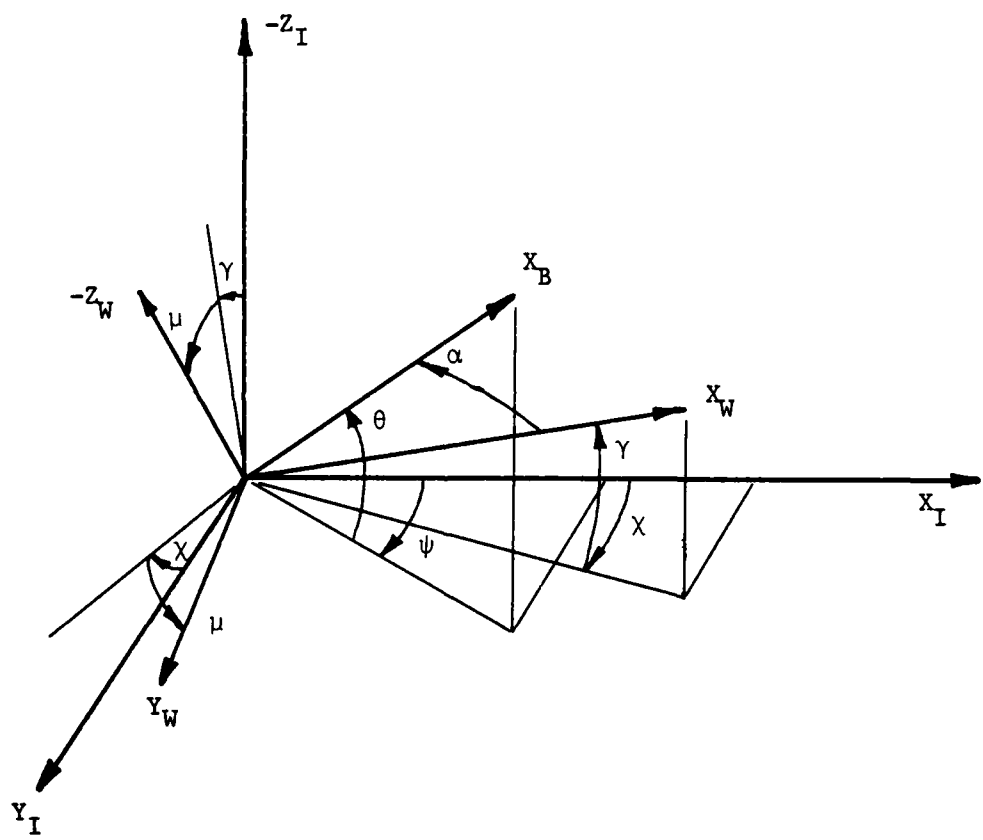


Figure 1. Missile Axis Systems.

the relationship between the body axes and the inertial axes is given by

$$\begin{bmatrix} i_B \\ j_B \\ k_B \end{bmatrix} = T_2 T_1 \begin{bmatrix} i_I \\ j_I \\ k_I \end{bmatrix} . \quad (5)$$

Performing the multiplication leads to

$$T_3 = T_2 T_1 \quad (6)$$

where

$$T_3 = \begin{bmatrix} \cos\alpha\cos\gamma\cos\chi & \cos\alpha\cos\gamma\sin\chi & -\cos\alpha\sin\gamma \\ -\sin\alpha\cos\mu\sin\gamma\cos\chi & -\sin\alpha\cos\mu\sin\gamma\sin\chi & -\sin\alpha\cos\mu\cos\gamma \\ -\sin\alpha\sin\mu\sin\chi & +\sin\alpha\sin\mu\cos\chi & \\ \sin\mu\sin\gamma\cos\chi & \sin\mu\sin\gamma\sin\chi & \sin\mu\cos\gamma \\ -\cos\mu\sin\chi & +\cos\mu\cos\chi & \\ \\ \sin\alpha\cos\gamma\cos\chi & \sin\alpha\cos\gamma\sin\chi & -\sin\alpha\sin\gamma \\ +\cos\alpha\cos\mu\sin\gamma\cos\chi & +\cos\alpha\cos\mu\sin\gamma\sin\chi & +\cos\alpha\cos\mu\cos\gamma \\ +\cos\alpha\sin\mu\sin\chi & -\cos\alpha\sin\mu\cos\chi & \end{bmatrix} . \quad (7)$$

Equations (3) and (5) must be equal transformations. By setting the components equal, the equations for μ and α are found to be

$$\tan\mu = \frac{\cos\theta\sin(\psi-\chi)}{\sin\theta\cos\gamma - \cos\theta\cos(\psi-\chi)\sin\gamma} \quad (8)$$

$$\tan\alpha = \frac{(\sin\theta\cos\gamma - \cos\theta\cos(\psi-\chi)\sin\gamma)\cos\mu + \cos\theta\sin(\psi-\chi)\sin\mu}{\cos\theta\cos(\psi-\chi)\cos\gamma + \sin\theta\sin\gamma}. \quad (9)$$

2.3 Target System.

For this problem, the target is simply assumed to be a point mass with position and velocity components in inertial space.

2.4 Launch Geometry.

Figure 2 shows a view of the launch geometry. At launch, the missile is assumed to be on the negative Z_I axis with the body axis system parallel to the inertial axis system. The target initial position is determined by the initial range and the off-boresight angle, BAY, from the missile. Target direction is determined by the initial aspect angle, AAY. This angle is defined to be the angle between the target velocity vector and the line of sight between the missile and target. The missile and target are assumed to be co-altitude and co-velocity at launch.

After launch the inertial axis system remains stationary. The target remains at the launch altitude, but the missile is free to maneuver in any direction. Figure 3 shows a representation of the intercept geometry. The relative distances between the missile and target are also shown. The two inertial angular measurements are the

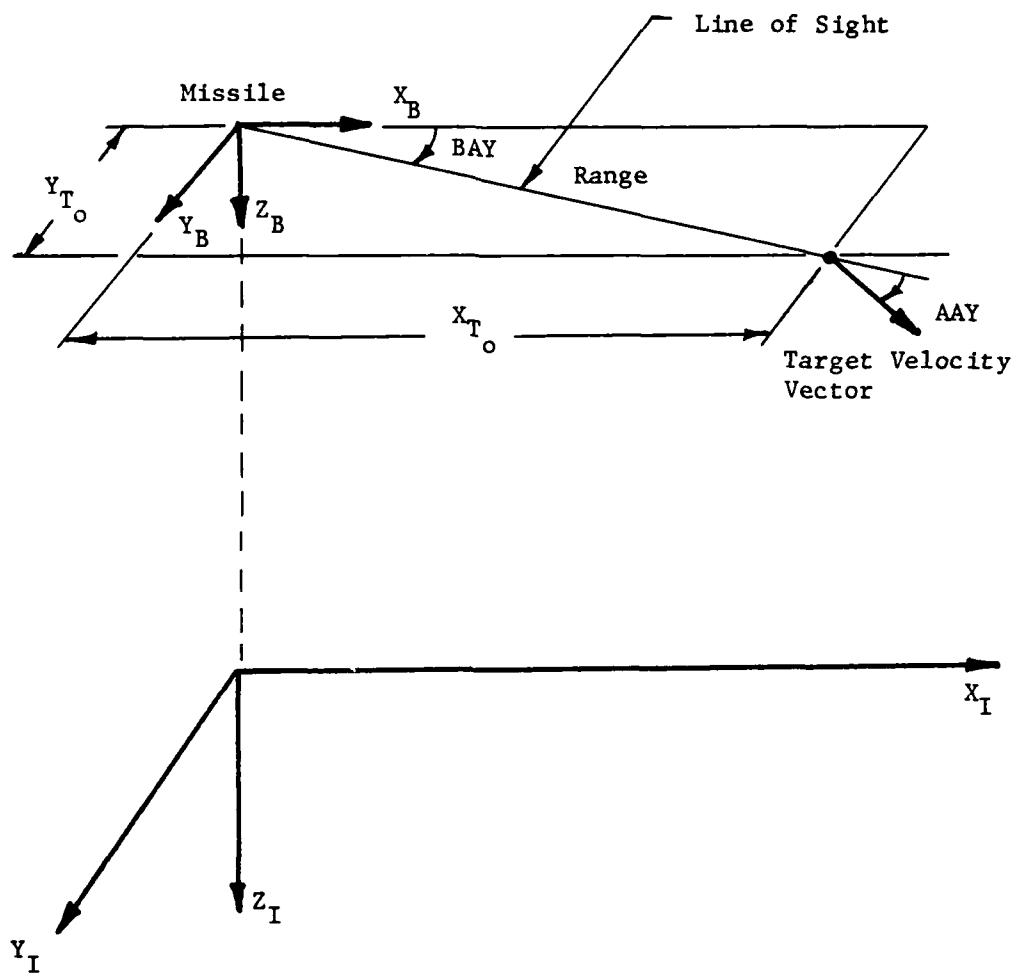


Figure 2. Launch Geometry.

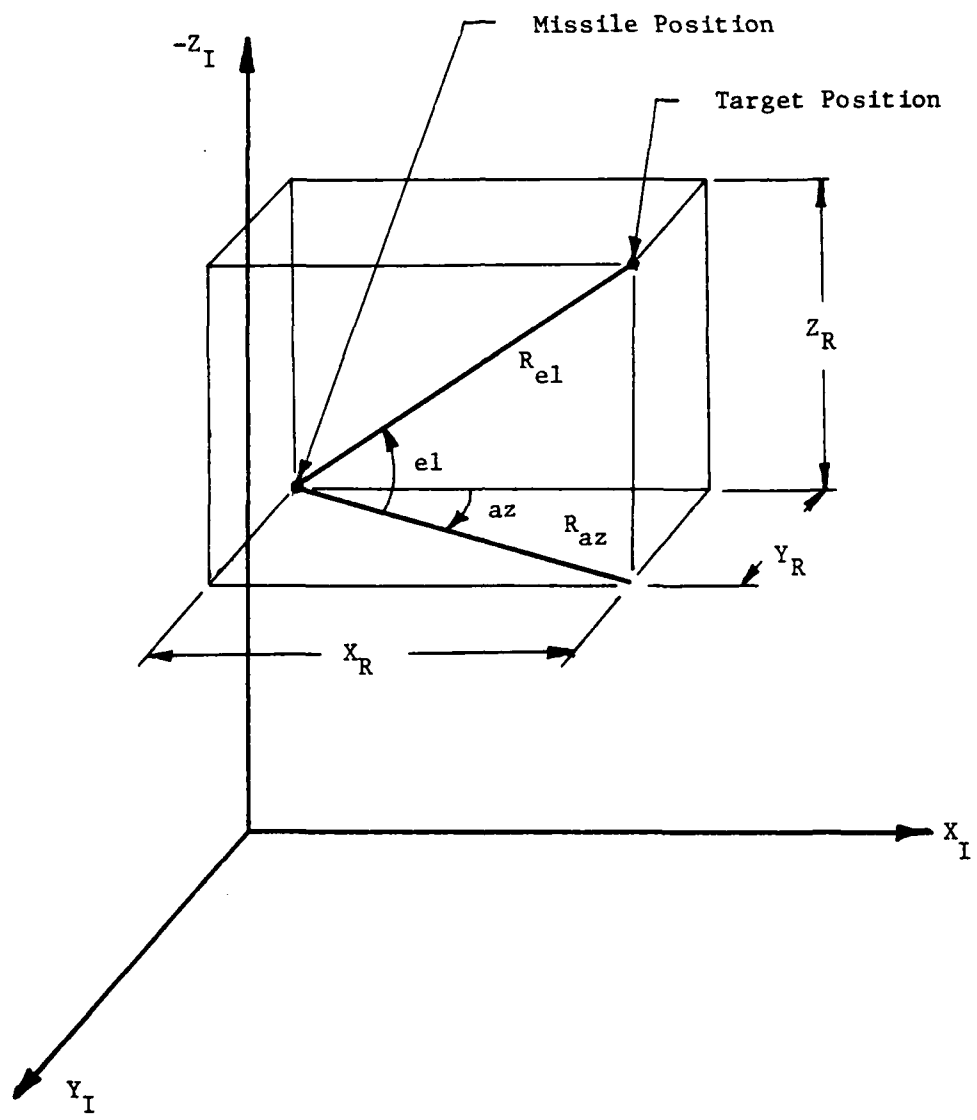


Figure 3. Intercept Geometry and Measurement Angles.

azimuth az and the elevation el of the target with respect to the missile. These angles are defined by the relative distances as follows

$$\begin{aligned} az &= \tan^{-1}(y_R/x_R) \\ el &= \tan^{-1}(-z_R/(x_R^2 + y_R^2)^{1/2}). \end{aligned} \tag{10}$$

SECTION III

MODELS

This section defines the missile model and all of its components, the target model, and the standard atmosphere.

3.1 Missile Model.

The missile model used is the three degree of freedom version of the model derived in Reference 2. Here, the missile is assumed to be able to instantly assume whatever body angles ψ and θ are commanded by the parameter optimization routine. Since it is the trajectory that is being optimized, it is assumed that this trajectory can be commanded perfectly by an autopilot; therefore there is no autopilot. Contributions made by the control surface deflections, by sideslip, and by moments of inertia are assumed to be negligible.

The missile launch takes place at $t = 0$ in accordance with the geometry in Section 2.4. The missile is not allowed to guide for the first .4 second, so for this time period the control angles are zero. At the end of this delay the missile is allowed to assume any position commanded by the optimization routine.

The differential equations of motion for the missile are as developed in Reference 4 for flight over a flat earth:

$$\begin{aligned}
 \dot{x}_1 &= \dot{x}_M = V_M \cos \gamma \cos \chi \\
 \dot{x}_2 &= \dot{y}_M = V_M \cos \gamma \sin \chi \\
 \dot{x}_3 &= \dot{z}_M = -V_M \sin \gamma \\
 \dot{x}_4 &= \dot{v}_M = (T \cos \alpha - D - W \sin \gamma) / m \\
 \dot{x}_5 &= \dot{\gamma} = ((T \sin \alpha + L) \cos \mu - W \cos \gamma) / V_M^m \\
 \dot{x}_6 &= \dot{\chi} = (T \sin \alpha + L) \sin \mu / (V_M^m \cos \gamma)
 \end{aligned} \tag{11}$$

where

$$\begin{aligned}
 T &= f(t) \\
 W &= f(t) \\
 m &= W/g \\
 D &= f(\alpha, V_M, Z_M) \\
 L &= f(\alpha, V_M, Z_M) \\
 \alpha &= f(\chi, \gamma, \psi, \theta) \\
 \mu &= f(\chi, \gamma, \psi, \theta) \\
 g &= \text{acceleration due to gravity, assumed constant.}
 \end{aligned} \tag{12}$$

The functions for α and μ were discussed in Section 2. The models for thrust, weight, drag and lift remain to be developed.

3.1.1 Thrust and Weight Models. The missile weighs 165 lb at launch. The propellant (50 lb) burns at an assumed constant mass flow rate for 2.6 seconds. During the burn, the thrust is assumed to be constant, 4711.5 lb. There is no other contribution to weight loss during the missile's time of flight. The thrust and weight profiles are

described by the expressions

$$T = \begin{cases} 4711.5 \text{ lb} & 0 \leq t \leq 2.6 \text{ sec} \\ 0 & 2.6 < t \end{cases} \quad (13)$$

$$W = \begin{cases} (165 - 19.23t) \text{ lb} & 0 \leq t \leq 2.6 \text{ sec} \\ 115 \text{ lb} & 2.6 < t \end{cases} \quad (14)$$

3.1.2 Aerodynamics Model. The components of the missile aerodynamic forces along the X_B and Z_B axes are given by the equations

$$F_X = -(C_{a_0} + C_{X\alpha} \alpha + C_{X\alpha^2} \alpha^2) \frac{1}{2} \rho v_M^2 S \quad (15)$$

$$F_Z = -(C_{N_{0T}} + C_{N\alpha} \alpha) \frac{1}{2} \rho v_M^2 S$$

where S is the missile reference area. The atmospheric density ρ is calculated using a standard atmosphere model.

The aerodynamic coefficients in Equations (15) are found by table look-up and linear interpolation. The values are listed in Tables 1 and 2. These tables and the interpolation routines have been taken directly from Reference 2. Drag and lift are then calculated from Equations (15) in accordance with Figure 4.

$$D = F_X \cos\alpha - F_Z \sin\alpha \quad (16)$$

$$L = -F_Z \cos\alpha + F_X \sin\alpha$$

TABLE 1. AERODYNAMIC COEFFICIENTS, FUNCTIONS OF M

M	0.0	0.8	0.95	1.1	1.3	1.51	2.5	3.5	6.0
C_{a_0}	.139	.139	.240	.320	.289	.264	.20	.179	.165
C_{X_α}	.0057	.0057	.0062	.0068	.0064	.0051	.0034	.0011	.0011
$C_{X_\alpha^2}$	-.00061	-.00061	-.00043	-.00032	-.00029	-.00015	.00002	.000011	.00001

TABLE 2. AERODYNAMIC COEFFICIENT, $C_N(\alpha, M)$

$\alpha \backslash M$	0.0	.8	.95	1.1	1.3	1.51	2.5	3.5	6.0
0.	0.0	0.0	0.0	0.0	0.0	0.0	0.0	0.0	0.0
2.	.621	.621	.679	.703	.650	.561	.413	.339	.339
4.	1.555	1.333	1.448	1.479	1.361	1.182	.848	.686	.339
8.	2.903	2.903	3.207	3.198	2.869	2.470	1.764	1.398	1.398
12.	4.533	4.533	5.013	4.887	4.374	3.851	2.701	2.145	2.145
16.	6.082	6.082	6.831	6.574	5.917	5.158	3.658	2.942	2.942
20.	6.894	6.894	7.488	8.105	7.373	6.472	4.689	3.810	3.810

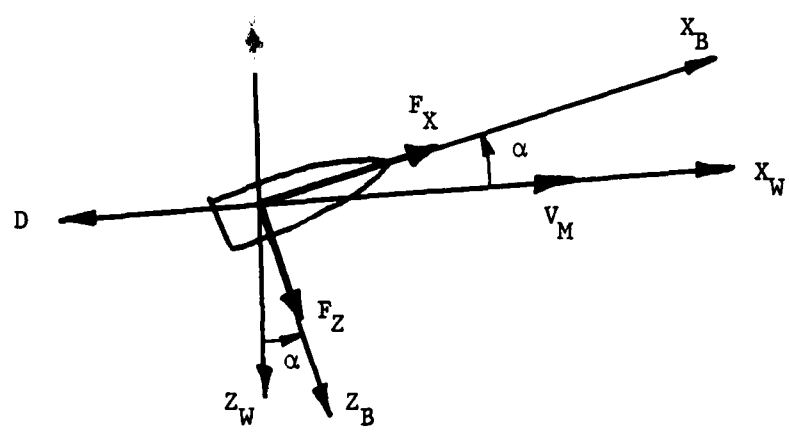


Figure 4. Lift and Drag.

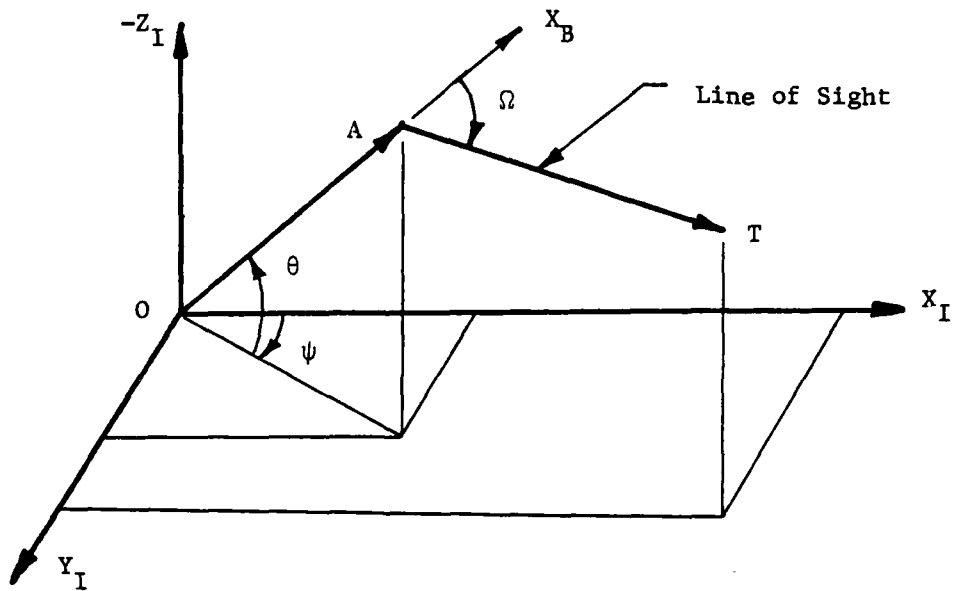


Figure 5. Boresight Angle.

3.1.3 Seeker Model. The actual seeker and how it works is not modeled. However, to simulate the presence of a seeker, a limit is imposed on the angle between the positive X_B axis and the line of sight to the target. This angle, shown in Figure 5, is called the boresight angle and is limited to

$$|\Omega| \leq 60^\circ. \quad (17)$$

This limit represents the maximum angle off boresight that the seeker can track the target. It is a physical limitation; if the boresight angle were to become greater than 60° , the seeker would break lock.

The boresight angle is found by using the definition of a dot product. From Figure 5, it is seen that

$$|\overline{OA}| |\overline{AT}| \cos\Omega = \overline{OA} \cdot \overline{AT} \quad (18)$$

where O represents the missile center of gravity, and A is the seeker gimbal pivot point. The inertial axis system shown is actually a parallel system through the missile c.g. T represents the target position.

A unit vector in the direction \overline{OA} can be defined using the Euler angles from Equation (3), that is,

$$\overline{OA}/|\overline{OA}| = (i_I \cos\theta \cos\psi + j_I \cos\theta \sin\psi - k_I \sin\theta). \quad (19)$$

The vector \overline{AT} is the relative range vector

$$\overline{AT} = X_R i_I + Y_R j_I + Z_R k_I \quad (20)$$

where X_R , Y_R , and Z_R are the relative ranges in the X_I , Y_I , and Z_I directions respectively (see Figure 3). The boresight angle is then found to be

$$\cos\Omega = \frac{X_R \cos\theta\cos\psi + Y_R \cos\theta\sin\psi - Z_R \sin\theta}{(X_R^2 + Y_R^2 + Z_R^2)^{\frac{1}{2}}} \quad (21)$$

3.1.4 Accelerometer Model. The normal acceleration is limited to a maximum of 100 g's. Missile normal acceleration is modeled by

$$a_{Z_B} = F_Z / W \quad (22)$$

where F_Z is the component of aerodynamic force along the Z_B axis as defined in Equations (15), and W is the weight from Equation (14). The limit, for structural reasons, is

$$|a_{Z_B}| \leq 100 \text{ g's} \quad (23)$$

3.2 Target Model.

The target is considered to be a non-maneuvering, non-accelerating, point mass moving through inertial space. Therefore, the target model consists of only the three inertial position components

$$\begin{aligned} X_T &= X_{T_0} + V_{T_x} t \\ Y_T &= Y_{T_0} + V_{T_y} t \\ Z_T &= Z_{T_0} \end{aligned} \quad (24)$$

For this problem, the velocity components are as follows:

$$\begin{aligned} V_{T_x} &= V_T \cos(AAY + BAY) \\ V_{T_y} &= V_T \sin(AAY + BAY) \\ V_{T_z} &= 0 \end{aligned} \quad (25)$$

where V_T is the constant target velocity and AAY and BAY are the initial aspect angle and off-boresight angle, respectively, as defined in Section 2.4.

3.3 Atmospheric Model.

The atmospheric model is needed to compute the speed of sound and the density for a given altitude. This model is a standard, constant gravity atmosphere for the troposphere (0 to 36089 ft) and the stratosphere (36089 to 82021 ft). It is the same model developed in Reference 2.

SECTION IV
THE INFORMATION MATRIX

In Reference 1, a dynamical system used in an onboard, optimal filter to estimate relative position, relative velocity, and target acceleration is presented. In order to measure the observability of the state estimate which can be made from this dynamical system and measurement function, the information matrix is used. In this section, the information matrix and measures associated with the information matrix are developed as the performance criteria for the optimization problem.

4.1 Definition.

The information matrix is defined by Reference 5 as

$$I(t, t_0) \triangleq \int_{t_0}^t \Phi^T(\tau, t) H^T(\tau) V^{-1}(\tau) H(\tau) \Phi(\tau, t) d\tau \quad (26)$$

where $\Phi(\tau, t)$ is the state transition matrix used by the filter. $H(\tau)$ is the matrix of partial derivatives of the measurement function with respect to the state variables evaluated on the nominal path, and $V(\tau)$ is the measurement noise power spectral density. Each of these elements will be discussed in this section.

The information matrix is related to the inverse of the error covariance matrix $P^{-1}(t)$. If it is assumed that there is no process

noise, for any time period t_i to t_j , the information matrix is given by

$$I(t_j, t_i) = P^{-1}(t_j) - \Phi^T(t_0, t_j) P_0^{-1} \Phi(t_0, t_j) \quad (27)$$

where P_0 is the a priori error covariance (Reference 6). If there is no a priori information, i.e., if $P_0^{-1} = 0$,

$$I(t_j, t_i) = P^{-1}(t_j). \quad (28)$$

The larger the eigenvalues of the information matrix, the smaller the eigenvalues of the corresponding error covariance matrix will be, and the more precise the estimate will be. This is the basis for using the information matrix as the performance index. The trajectory which maximizes the eigenvalues of the information matrix is also the trajectory which gives the most precise estimate.

A scalar is needed for the performance index. The two operations available are the trace and determinant. The trace is equal to the sum of the eigenvalues of a matrix; the determinant is equal to the product of the eigenvalues. Because of its simplifying characteristics, primarily that the trace and integration operations are interchangeable, the trace of the information matrix has been chosen. Since this is an optimization problem solved on a finite word length computer, a constant weighting matrix is included to normalize the terms in the trace. This weighting matrix does change the eigenvalues, but since it is a constant, the maximizing has the same effect.

The performance index now becomes

$$\begin{aligned} J &= \text{tr } W I (t_f, t_0) \\ &= \text{tr } W \int_{t_0}^{t_f} \Phi^T(\tau, t_f) H^T(X(\tau)) V^{-1}(\tau) H(X(\tau)) \Phi(\tau, t_f) d\tau. \end{aligned} \quad (29)$$

Since the trace and the integral operations are interchangeable and the weighting matrix is a constant, J can be rewritten as

$$J = \int_{t_0}^{t_f} \text{tr}(W \Phi^T(\tau, t_f) H^T(X(\tau)) V^{-1}(\tau) H(X(\tau)) \Phi(\tau, t_f)) d\tau. \quad (30)$$

This defines the form of the performance index used for this problem.

The elements of this equation remain to be defined.

4.2 The Dynamical System.

The dynamical system used by the filter (Reference 1) is of the form

$$\dot{X}(t) = F X(t) + G u(t) \quad (31)$$

$$z(t) = g(X(t)) + v(t). \quad (32)$$

The dynamics equation (Equation 31) is linear in rectangular coordinates. X is a nine-state vector of relative position, relative velocity and target acceleration given by

$$\mathbf{X} = [x_R \ y_R \ z_R \ u_R \ v_R \ w_R \ a_{T_X} \ a_{T_Y} \ a_{T_Z}]^T \quad (33)$$

where

$$\begin{aligned} x_R &= x_R(t) = x_T(t) - x_M(t) \\ y_R &= y_R(t) = y_T(t) - y_M(t) \\ z_R &= z_R(t) = z_T(t) - z_M(t) \\ u_R &= u_R(t) = v_{T_X}(t) - v_{M_X}(t) \\ v_R &= v_R(t) = v_{T_Y}(t) - v_{M_Y}(t) \\ w_R &= w_R(t) = v_{T_Z}(t) - v_{M_Z}(t), \end{aligned} \quad (34)$$

and a_{T_X} , a_{T_Y} , and a_{T_Z} are the inertial target acceleration components.
Equation (31) in scalar form is

$$\begin{aligned} \dot{x}_R &= u_R \\ \dot{y}_R &= v_R \\ \dot{z}_R &= w_R \\ \dot{u}_R &= a_{T_X} - a_{M_X} \\ \dot{v}_R &= a_{T_Y} - a_{M_Y} \\ \dot{w}_R &= a_{T_Z} - a_{M_Z} \\ \dot{a}_{T_X} &= -\lambda a_{T_X} \\ \dot{a}_{T_Y} &= -\lambda a_{T_Y} \\ \dot{a}_{T_Z} &= -\lambda a_{T_Z}, \end{aligned} \quad (35)$$

where λ is a target acceleration constant. The control, $u(t)$, is assumed known, and consists of the three missile inertial acceleration components, a_{M_X} , a_{M_Y} , and a_{M_Z} . From Equation (35) it can be seen that the matrix F from Equation (31) is

$$F = \begin{bmatrix} 0 & I & 0 \\ - & \Gamma & \Gamma \\ 0 & 0 & I \\ - & \Gamma & \Gamma \\ 0 & 0 & -\lambda \end{bmatrix}, \quad (36)$$

and the matrix G is

$$G = \begin{bmatrix} 0 & 0 & 0 \\ - & \Gamma & \Gamma \\ 0 & -I & 0 \\ - & \Gamma & \Gamma \\ 0 & 0 & 0 \end{bmatrix}, \quad (37)$$

where each partition is 3×3 , I is the identity matrix, and λ is a diagonal matrix of the target acceleration constants.

The measurement equation (Equation (32)) is nonlinear in rectangular coordinates. The measurement z is a two-dimensional angle measurement, $g(X)$ is the measurement function, and $v(t)$ is a zero mean, white noise process associated with the measurement, with power spectral density $V(t)$. The measurement function consists of the two inertial angle measurements for azimuth and elevation (see Figure 3)

$$g(X(t)) = \begin{bmatrix} \tan^{-1}(Y_R/X_R) \\ \tan^{-1}(-Z_R/(X_R^2 + Y_R^2)^{1/2}) \end{bmatrix}. \quad (38)$$

The linearized measurement equation is

$$\delta z(t) = H(X(t))\delta X + v(t), \quad (39)$$

where $H(X(t))$ is the partial of g with respect to X evaluated on the nominal path. The elements of H are

$$H(X(t)) = \begin{bmatrix} g_{1X_1} & g_{1X_2} & 0 & 0 & 0 & 0 & 0 & 0 \\ g_{2X_1} & g_{2X_2} & g_{2X_3} & 0 & 0 & 0 & 0 & 0 \end{bmatrix} \quad (40)$$

where

$$\begin{aligned} H_{11} &= g_{1X_1} = -\frac{Y_R}{R_{az}} \\ H_{12} &= g_{1X_2} = \frac{X_R}{R_{az}} \\ H_{21} &= g_{2X_1} = \frac{X_R Z_R}{R_{el}^2} \cdot \frac{1}{R_{az}} \\ H_{22} &= g_{2X_2} = \frac{Y_R Z_R}{R_{el}^2} \cdot \frac{1}{R_{az}} \\ H_{23} &= g_{2X_3} = -\frac{R_{az}}{R_{el}^2} \end{aligned}, \quad (41)$$

where

$$R_{az} = R_{az}(t) = (X_R^2 + Y_R^2)^{\frac{1}{2}} \quad (42)$$

$$R_{el} = R_{el}(t) = (X_R^2 + Y_R^2 + Z_R^2)^{\frac{1}{2}},$$

as shown in Figure 3.

4.3 The State Transition Matrix.

Because of the simplicity of the matrix F (Equation (36)), the state transition matrix has been derived in closed form. The elements of $\Phi(t, \tau)$ are given by (Reference 1)

where

$$\begin{aligned}
 \Phi_{11}(t, \tau) &= \Phi_{22}(t, \tau) = \Phi_{33}(t, \tau) = 1 \\
 \Phi_{44}(t, \tau) &= \Phi_{55}(t, \tau) = \Phi_{66}(t, \tau) = 1 \\
 \Phi_{14}(t, \tau) &= \Phi_{25}(t, \tau) = \Phi_{36}(t, \tau) = t - \tau \stackrel{\Delta}{=} \Delta t \\
 \Phi_{77}(t, \tau) &= \Phi_{88}(t, \tau) = \Phi_{99}(t, \tau) = \exp(-\lambda \Delta t) \\
 \Phi_{47}(t, \tau) &= \Phi_{58}(t, \tau) = \Phi_{69}(t, \tau) = -\frac{1}{\lambda}(\exp(-\lambda \Delta t) - 1) \\
 \Phi_{17}(t, \tau) &= \Phi_{28}(t, \tau) = \Phi_{39}(t, \tau) = \frac{1}{\lambda^2}(\exp(-\lambda \Delta t) + \lambda \Delta t - 1)
 \end{aligned} \tag{44}$$

and where λ is the target acceleration constant (Reference 1).

Since the information matrix requires $\Phi(\tau, t)$, the identity for the inverse of a state transition matrix

$$\Phi(\tau, t) = \Phi^{-1}(t, \tau) \tag{45}$$

can be used. Hence, the elements of $\Phi(\tau, t)$ are

$$\begin{aligned}
 \Phi_{11}(\tau, t) &= \Phi_{22}(\tau, t) = \Phi_{33}(\tau, t) = 1 \\
 \Phi_{44}(\tau, t) &= \Phi_{55}(\tau, t) = \Phi_{66}(\tau, t) = 1 \\
 \Phi_{14}(\tau, t) &= \Phi_{25}(\tau, t) = \Phi_{36}(\tau, t) = \tau - t = -\Delta t \\
 \Phi_{77}(\tau, t) &= \Phi_{88}(\tau, t) = \Phi_{99}(\tau, t) = \exp(\lambda \Delta t) \\
 \Phi_{47}(\tau, t) &= \Phi_{58}(\tau, t) = \Phi_{69}(\tau, t) = -\frac{1}{\lambda}(\exp(\lambda \Delta t) - 1) \\
 \Phi_{17}(\tau, t) &= \Phi_{28}(\tau, t) = \Phi_{39}(\tau, t) = \frac{1}{\lambda^2}(\exp(\lambda \Delta t) + \lambda \Delta t - 1)
 \end{aligned} \tag{46}$$

4.4 Angle Measurement Noise.

The matrix $V(t)$ is a 2×2 matrix representing the power spectral density of the angle measurements due to certain target-sensor characteristics, that is,

$$V(t) = \begin{bmatrix} V_{11}(t) & 0 \\ 0 & V_{22}(t) \end{bmatrix}$$

$$V_{11}(t) = \frac{a}{R_{az}^2} + b$$

$$V_{22}(t) = \frac{a}{R_{el}^2} + b . \quad (47)$$

$V_{11}(t)$ denotes the power spectral density associated with measuring azimuth and $V_{22}(t)$ denotes the power spectral density associated with measuring elevation. The term a is a constant associated with the received signal power noise. The term b represents the uncertainty in target position, possibly due to atmospheric refraction of the signal to the sensor and fading. For this problem,

$$\begin{aligned} a &= .25 \text{ rad}^2 \text{ ft}^2 \text{ sec} \\ b &= 56.25 \times 10^{-8} \text{ rad}^2 \text{ sec} \end{aligned} \quad (48)$$

are typical values for current sensors.

$V(t)$ may be simplified by factoring out a , that is,

$$V(t) = a \begin{bmatrix} \frac{1}{R_{az}^2} + c & 0 \\ 0 & \frac{1}{R_{el}^2} + c \end{bmatrix}, \quad (49)$$

where $c = b/a$.

4.5 Weighting Matrix.

The weighting matrix W is a constant, 9×9 diagonal matrix used to give relative, equal values to the terms in the information matrix. The off-diagonal terms are all zero, while the diagonal terms are defined as follows:

$$\begin{aligned} W_{11} &= W_{22} = W_{33} \stackrel{\Delta}{=} W_1 = 1 \\ W_{44} &= W_{55} = W_{66} \stackrel{\Delta}{=} W_2 = t_f^{-2} \\ W_{77} &= W_{88} = W_{99} \stackrel{\Delta}{=} W_3 = e^{-2t_f}. \end{aligned} \quad (50)$$

W_1 , W_2 , and W_3 weight the position terms, the velocity terms and the target acceleration terms, respectively. They have been chosen in an effort to get the maximum numerical value of each of these terms to be approximately equal to one. Without this relative weighting, the target acceleration terms completely dominate the other factors. This becomes obvious in Section 4.6 where the performance index is

simplified, and the effects of the weights can be seen.

4.6 The Performance Index.

After multiplying out the terms in Equation (30) and performing the trace operation inside the integral, J becomes

$$\begin{aligned} J = & \int_{t_0}^{t_f} ((\Phi_{11} \text{HH}_1 \Phi_{11} + \Phi_{22} \text{HH}_2 \Phi_{22} + \Phi_{33} \text{HH}_3 \Phi_{33}) w_1 \\ & + (\Phi_{14} \text{HH}_1 \Phi_{14} + \Phi_{25} \text{HH}_2 \Phi_{25} + \Phi_{36} \text{HH}_3 \Phi_{36}) w_2 \\ & + (\Phi_{17} \text{HH}_1 \Phi_{17} + \Phi_{28} \text{HH}_2 \Phi_{28} + \Phi_{39} \text{HH}_3 \Phi_{39}) w_3) d\tau \quad (51) \end{aligned}$$

where $\Phi = \Phi(\tau, t_f)$, and where

$$\begin{aligned} \text{HH}_1 &= \text{HH}_1(\tau) = \frac{g_1^2(\tau)}{v_{11}(\tau)} + \frac{g_2^2(\tau)}{v_{22}(\tau)} \\ \text{HH}_2 &= \text{HH}_2(\tau) = \frac{g_1^2(\tau)}{v_{11}(\tau)} + \frac{g_2^2(\tau)}{v_{22}(\tau)} \quad (52) \\ \text{HH}_3 &= \text{HH}_3(\tau) = \frac{g_1^2(\tau)}{v_{11}(\tau)} . \end{aligned}$$

The performance index further simplifies to

$$J = \frac{1}{a} \int \frac{t_f}{t_0} \left\{ \left[\frac{1}{1 + cR_{az}^2} + \frac{1}{1 + cR_{el}^2} \right] \cdot \left[w_1 \Phi_{11}^2 + w_2 \Phi_{14}^2 + w_3 \Phi_{17}^2 \right] \right\} d\tau. \quad (53)$$

SECTION V
PROBLEM FORMULATION

This section formulates the problem as an optimal control problem and presents all of the constraints. The problem is then converted to a parameter optimization problem.

5.1 The Optimal Control Problem.

The objective is to find the control which maximizes the information, completes the air-to-air intercept (zero miss distance), and satisfies all of the dynamical, physical, and aerodynamic constraints, that is,

Maximize Equation (53) (54)

subject to the terminal constraint of zero miss distance and the system model developed in Section 3. The dynamical part of this model takes the form of differential constraints and is nonlinear in the form

$$\dot{x} = f(t, x, u) \quad (55)$$

where the control u consists of the body angles ψ and θ .

The initial conditions x_0 for the differential equations of the missile are

$$\begin{aligned}
 x_1(0) &= 0 \\
 x_2(0) &= 0 \\
 x_3(0) &= -h_0 \\
 x_4(0) &= v_{M_0} \\
 x_5(0) &= 0 \\
 x_6(0) &= 0 ,
 \end{aligned} \tag{56}$$

where the values h_0 and v_{M_0} are input values for initial altitude and velocity.

The terminal constraint of zero miss distance is formulated as three equality constraints in the form

$$\Psi(t_f, x_f) = \begin{bmatrix} \Psi_1 \\ \Psi_2 \\ \Psi_3 \end{bmatrix} = \begin{bmatrix} (X_{T_f} - X_{M_f}) / X_{T_f} \\ (Y_{T_f} - Y_{M_f}) / Y_{T_f} \\ (Z_{T_f} - Z_{M_f}) / Z_{T_f} \end{bmatrix} , \tag{57}$$

where the values of Ψ denote the actual constraint residuals for the current control. The object is to drive these values to zero. X_T , Y_T , and Z_T are the target inertial position components. The subscript f denotes the condition at the final time.

The remaining constraints are due to physical or aerodynamic limitations and are formulated as inequality constraints, $\theta(t, x, u) \geq 0$.

The limitations are

$$\begin{aligned}
 t_f &\leq 8 \text{ sec} \\
 |a_{Z_B}| &\leq 100 \text{ g's} \\
 |\Omega| &\leq 60^\circ & (58) \\
 |\alpha| &\leq 20^\circ \\
 |\gamma| &\leq 80^\circ
 \end{aligned}$$

The final time is limited to no more than 8 seconds in order to ensure that the missile still has enough velocity to maneuver. The missile normal acceleration is limited to 100 g's for structural reasons. The missile seeker has a maximum angle limit of 60° off boresight, hence the constraint on boresight angle. Maximum angle of attack is 20° , as limited by the aerodynamics tables. The limit on the flight path angle is included to keep the equations of motion defined. The value of \dot{x} (Equations (11)) becomes infinite at $\gamma = 90^\circ$. Instead of re-defining the equations, a state inequality constraint is used to keep γ away from 90° because, it was felt, the final trajectory would not require γ above 80° . Until the converged solution is found, these inequality constraints may or may not be satisfied.

During the optimization process, the inequality constraints are evaluated according to their constraint residuals. For the final time constraint

$$\theta_1 = 1 - t_f / 8. \quad (59)$$

The remaining inequality constraints could be violated at any time from t_0 to t_f . Therefore, the constraint residuals are evaluated as integral constraints, that is,

$$\begin{aligned}
 \theta_2 &= - \int_{t_0}^{t_f} \left[\min((100 - |a_{M_{Z_B}}(t)|), 0) \right]^2 dt \\
 \theta_3 &= - \int_{t_0}^{t_f} \left[\min((60 - |\Omega(t)|), 0) \right]^2 dt \\
 \theta_4 &= - \int_{t_0}^{t_f} \left[\min((20 - |\alpha(t)|), 0) \right]^2 dt \\
 \theta_5 &= - \int_{t_0}^{t_f} \left[\min((80 - |\gamma(t)|), 0) \right]^2 dt .
 \end{aligned} \tag{60}$$

The performance index (Equation (54)) and the integral constraints are formulated as differential equations with zero initial values and evaluated along with the state differential equations. This augments the state vector (Equation (11)) by five: x_7 for the performance index, and x_8 through x_{11} for the integral constraint residuals. The values of the performance index and the integral constraint residuals (Equation (60)) are the values of the augmented state variables at the final time, that is,

$$\begin{aligned}
 J &= x_7_f \\
 \theta_2 &= x_8_f & \theta_4 &= x_{10_f} \\
 \theta_3 &= x_{9_f} & \theta_5 &= x_{11_f} .
 \end{aligned} \tag{61}$$

5.2 The Parameter Optimization Method.

The preceding forms an optimal control problem to find the control $u(t)$ which maximizes the performance index. To solve this, the problem is converted to a parameter optimization problem where the constraints are handled by penalty functions.

The problem of having a free final time is converted to a fixed, normalized final time by defining a new independent variable.

$$\tau = t / t_f \quad (62)$$

or

$$\begin{aligned} t &= t_f \tau \\ dt &= t_f d\tau. \end{aligned} \quad (63)$$

Thus, the equations of motion become

$$\frac{dx}{dt} = \frac{dx}{t_f d\tau} = f(t_f \tau, x, u) \quad (64)$$

or

$$\frac{dx}{d\tau} = g(\tau, x, u, t_f) , \quad (65)$$

where $\tau_0 = 0$, $\tau_f = 1$. Final time is now a parameter to be found along with the control. The control is now a function of τ , the new

independent variable.

The continuous control function is approximated by two cubic splines, one for each control, with unknown parameters, that is,

$$u = u(a, \tau) , \quad (66)$$

where a is a vector of n unknown parameters

$$a = [a_1 \ a_2 \ \dots \ a_n]^T. \quad (67)$$

For each control function these parameters are the values of the control at $\tau = 0$, $\tau = \frac{1}{2}$, $\tau = 1$, and the slope at each end point. For any value of a , a cubic spline is fit to the parameters, and the control can be found for any τ between 0 and 1.

The parameters to optimize now are the final time and the parameters of the cubic splines which define the control function. They can be lumped together as one vector of length $n + 1$

$$b = [t_f \ a]^T. \quad (68)$$

From Equations (65), (66), and (68), it can be seen that $x_f = x_f(b)$. Therefore, since the performance index is a function of x_f and t_f , J can now be written

$$J \stackrel{\Delta}{=} \phi(b) \quad (69)$$

where $\phi(b) = -x_7 f$.

The problem can now be restated as

$$\text{Minimize } J = \phi(b) \quad (70)$$

subject to

$$\begin{aligned} \Psi(b) &= 0 \\ \theta(b) &\geq 0, \end{aligned} \quad (71)$$

where

$$\begin{aligned} b &= \begin{bmatrix} t_f & a \end{bmatrix}^T \\ u &= u(a, \tau). \end{aligned} \quad (72)$$

SECTION VI
SOLUTION METHOD

This section gives a brief description of the problem solution method.

6.1 Input.

The input required for this program is initial missile and target positions and an initial set of parameters, b . The missile and target are set up as described in Section 2. An initial altitude, velocity, range, off-boresight angle and aspect angle must be specified. The control is represented by two cubic splines, one for each control angle. Each spline function is assumed to have 5 parameters - the control angles at $\tau = 0$, $\tau = \frac{1}{2}$, and at $\tau = 1$, and the slope at each end point. Since t_f is also a parameter, a total of 11 parameters must be input.

6.2 Optimization Method.

The optimization method used is a penalty function-Lagrange multiplier method which is completely developed in Reference 3. The penalty function used is

$$P(b, \beta, S) = \phi(b) + \frac{1}{2} \Gamma(b, \beta)^T S \Gamma(b, \beta). \quad (73)$$

Here, b is the $n + 1$ vector from Equation (69) which contains the

parameters to be optimized. $\Gamma(b)$ is an m vector where m is the total number of constraints, that is,

$$\Gamma(b, \beta) = \begin{cases} C_1(b) - \beta_1 & , 1 \leq i \leq k \\ \min(C_i(b) - \beta_i, 0) & , k+1 \leq i \leq m \end{cases} \quad (74)$$

where

$$C(b) = \begin{bmatrix} C_1 = \psi_1 \\ \vdots \\ C_k = \psi_k \\ C_{k+1} = \theta_1 \\ \vdots \\ C_m = \theta_{m-k} \end{bmatrix} \quad (75)$$

Hence, the first k elements of $C(b)$ are the equality constraint residuals, and elements $k+1$ to m are the inequality constraint residuals.

S is an $m \times m$ diagonal weighting matrix with elements σ_i , where i goes from 1 to m . The m vector β is used to allow convergence without the necessity of forcing S to infinity.

This is an iterative method where each iteration involves minimizing $P(b, \beta, S)$ for a fixed β and S using a variable-metric method for unconstrained optimization. After each iteration, β and S are varied in such a way that the parameters tend to the constrained solution.

The aim is to vary β so that, for a constant S , the value of the product

β S tends to the vector of Lagrange multipliers for the problem. The values σ_i are only increased in case the rate of convergence of the corresponding $C_i(b)$ to zero is not sufficiently rapid. Convergence is obtained when $|C_i(b)| \leq \epsilon_i$, for $1 \leq i \leq m$.

The computer subroutine incorporating this method was taken from the Harwell library and is named VF01A. To use VF01A, the user must supply a routine called VF01B which evaluates $\phi(b)$, $\nabla\phi(b)$, $C(b)$, and $\nabla C(b)$, where

$$\nabla\phi(b) = \frac{\partial\phi(b)}{\partial b_i} \quad (76)$$

$$\nabla C_{ij}(b) = \frac{\partial C_j(b)}{\partial b_i} \quad (77)$$

for $1 \leq i \leq (n+1)$ and $1 \leq j \leq m$.

6.3 Function Evaluation.

The function evaluation consists of finding the performance index $J = \phi(b)$, and the constraint violations, $C(b)$. These values are then used to form Equation (73). Figure 6 is a block diagram showing the elements of the program which handle the function evaluation. Each block represents a subroutine.

Subroutine SG is called from VF01B with the current set of parameters b . SG is the driving routine which sets all the initial conditions, calls the integrator, and then returns the values of ϕ

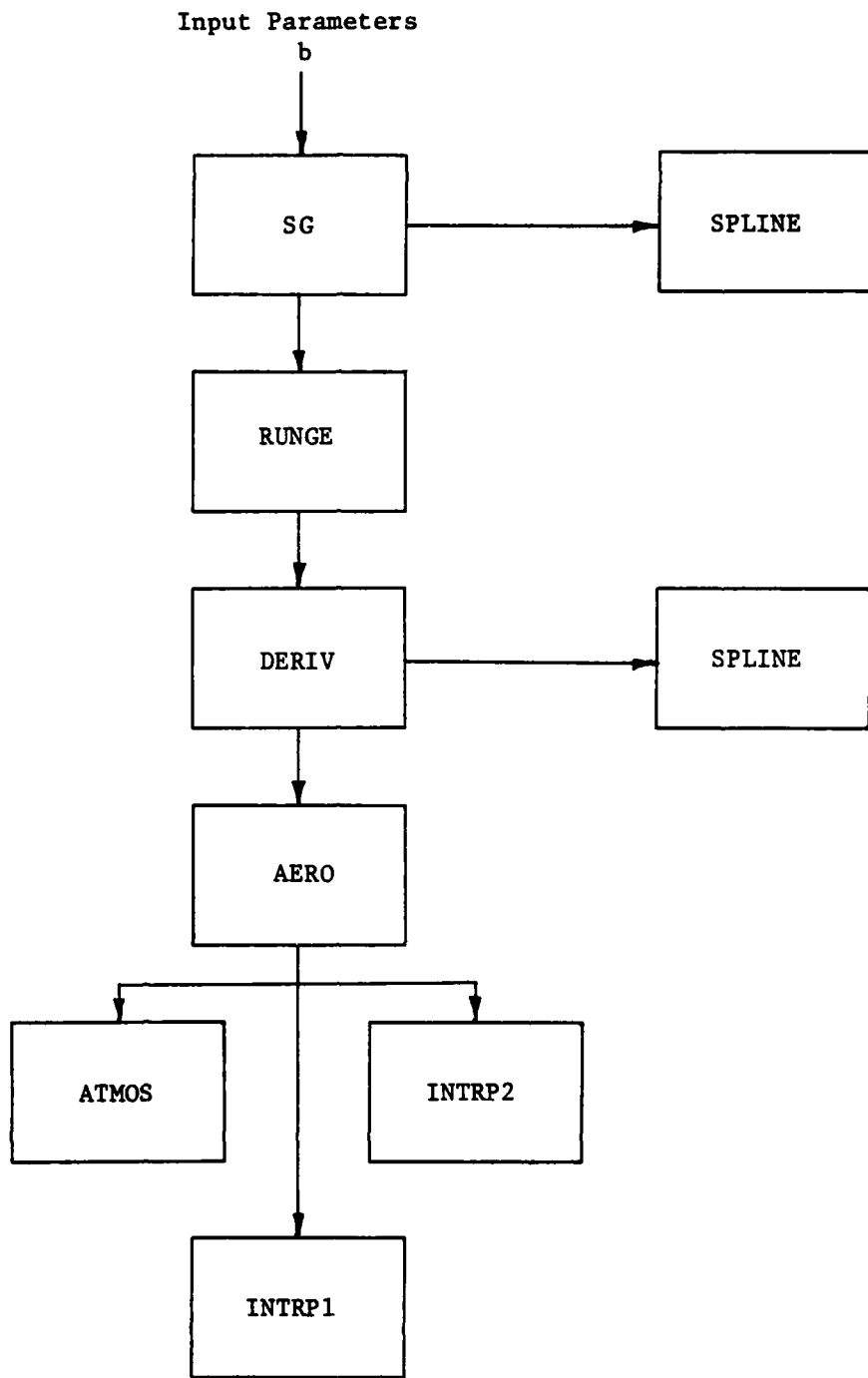


Figure 6. Function Evaluation.

and C. SPLINE is called immediately upon entry to SG to evaluate the coefficients of the cubic spline functions of the control for a fixed

b. The control can then be evaluated explicitly as a function of τ .

The integrator RUNGE is a fixed-step, fourth-order Runge-Kutta method. The system differential equations, the performance index, and the integral constraints are all integrated simultaneously.

The complete system model is contained in, or called by DERIV. For every time τ , DERIV finds the control by calling SPLINE and evaluates the differential equations. There are 11 differential equations: 6 for the state equations, 1 for the performance index, and 4 for the integral constraints. The aerodynamics tables required to evaluate drag and lift are contained in AERO. ATMOS, the standard atmosphere model, must be called to find the Mach number and the atmospheric density for the instantaneous altitude and velocity. The aerodynamic tables (Tables 1 and 2) are functions of Mach or of Mach and angle of attack. The routines used to linearly interpolate the aerodynamic coefficient tables are INTRP1 and INTRP2, respectively.

6.4 Numerical Derivatives.

To obtain $\nabla\phi(b)$ and $\nabla C(b)$ as required for VF01A, numerical derivatives are evaluated by the method of central differences. For any function $G(x)$, the numerical derivative with respect to the k^{th} variable, x_k , is found by the formula

$$\frac{\partial G}{\partial x_k} = \frac{G(x_k + \Delta x_k) - G(x_k - \Delta x_k)}{2\Delta x_k} \quad (78)$$

where

$$\Delta x_k = \begin{cases} |x_k| \varepsilon & , \quad x_k > \varepsilon \\ \varepsilon^2 & , \quad x_k \leq \varepsilon. \end{cases} \quad (79)$$

6.5 Optimization Algorithm.

The algorithm used for constrained, numerical optimization in VFOLIA is stated as follows:

1. Guess b .
2. Set initial values of S, β .
3. Minimize $P(b, \beta, S)$ with respect to b .
 - a. Obtain ϕ and C by calling function evaluation routine.
 - b. Obtain $\nabla\phi$ and ∇C by calling numerical derivative routine.
 - c. Evaluate $P(b, \beta, S)$ and $\partial P(b, \beta, S) / \partial b$.
 - d. Use variable metric method for unconstrained minimization.
4. If the final conditions are set to desired accuracy, go to 6.
5. Vary β , and S if necessary; to to 2.
6. Return to executive program.

SECTION VII

RESULTS

In this section the launch scenarios are described, and the results are discussed.

7.1 Launch Scenarios.

Three different launch scenarios have been chosen for the computation of optimal information trajectories. Each intercept is initiated at 10,000 ft altitude with the missile and target co-altitude and co-speed at .9 Mach. The scenarios differ in the launch range and aspect angle only, as the boresight angle is zero for all engagements. The engagements are initiated at 3000 ft, 0° aspect; 3000 ft, 30° aspect; and at 7000 ft, 60° aspect. The target for each intercept is flying straight and level and nonaccelerating.

In order to test the system model and for comparison purposes, one additional intercept has been run, that of minimum final time. This is done simply by replacing the performance index with

$$J = t_f . \quad (80)$$

Everything else remains the same. The launch for this intercept occurs at 3000 ft and 30° aspect angle.

7.2 Results and Conclusions.

Since the measurements for the dynamical system are angle measurements only, it is expected that to increase the information the missile needs to fly a path which keeps these angles changing. The optimal trajectories found with this method are consistent with this expectation. During the intercept, the missile "fishtails" and "porpoises" to the maximum extent possible without violating any constraints. The angle rates for the boresight angle and for the measurement angles are kept high during the entire intercept. The boresight angle tries to go from limit to limit.

Figures 8 through 24 present the results in graphical form for each of the intercept scenarios. The missile launch point is where $X_I = 0$, $Y_I = 0$, and $Z_I = -10,000$ ft. Since nothing can happen for the first .4 seconds, the plots show only the time period for $.4 \leq t \leq t_f$. The figures are grouped by intercept, each group containing all the results for each scenario. The first two figures in each group show the actual intercept and target trajectories projected onto the X_I-Y_I and the X_I-Z_I planes respectively. For the horizontal trajectories, the viewer is above the X_I-Y_I plane looking down; for the vertical trajectories, the viewer is on the positive Y_I axis side of the X_I-Z_I plane. The next four figures are for the boresight angle, the boresight angle rate, the azimuth and elevation (measurement) angles, and the azimuth and elevation angle rates, all plotted versus time.

The next 6 figures (Figures 25 through 30) present the same information for the minimum time trajectory. These are shown primarily for comparison with the best information trajectories, but they also

demonstrate the validity of the system model and the optimization process. The minimum time results are just what you would expect. The trajectory is an easy, but direct turn onto an intercept path which approaches a straight line. There is no variation in elevation. An abrupt, hard turn would induce more drag and, thus, make a longer intercept. For contrast, the best information trajectory is also shown on the minimum time trajectory plots.

Table 3 lists the solved intercept problems by engagements. Each problem has converged satisfactorily, and the miss distances are all within 1 foot of the point mass target. The only inequality constraint which acts on the converged solution is the maximum boresight angle. The values of the performance index are also listed, but the only ones that can be compared are the ones with the same initial geometry. For the 3000 ft, 30° launch, the performance index for the maximum information trajectory is much higher than for the minimum time trajectory, as it should be.

Note the high number of function evaluations and the amount of computer time required for the best information solutions. Because of this, it would be impossible to use this optimization process in an onboard computer for a guidance scheme. If something like this were desirable, however, it may be possible to streamline the process in some way. This is a possible area for further research. For example, the aerodynamics tables could be replaced by some approximating function, eliminating the table look-up and interpolation process.

Another possibility is to formulate an empirical formula for the guidance law which would approximate the best information

TABLE 3. INTERCEPT RESULTS

Range (ft)	Aspect (deg)	Initial Geometry	Flight Time (sec)	Performance Index	Miss Distance (ft)			Active Inequality Constraints	Total Function Evals	Computation Time (sec)
					X _R	Y _R	Z _R			
3000	0	4.56	11.6	.222	.151	.242	Ω		14950	2276
3000	30	5.96	19.3	.011	.306	.074	Ω		8878	1349
7000	60	8.00	22.4	.086	.004	.058	Ω		13685	2067
Minimum Time									-	-
3000	30	2.65	4.56	.004	.000	.000				

trajectory. The plots for the three intercepts show a definite similarity between the scenarios. On each intercept the missile appears to be attempting to do the same thing, limited only by its requirement to complete the intercept. If, after running more trajectories, this is found to be the case, then an empirical formula might be found.

Another possible area for future research on this project is to find out how the trajectories would differ if some information about the state is removed. For example, if W_3 in Equation (53) is set to zero, the best information trajectory without target acceleration information would be found. This is because the target acceleration terms in the state transition matrix would be blanked out. If, it is found that the optimal trajectory is satisfactory without the target acceleration information, then this information would not have to be estimated by the onboard filter for the guidance law.

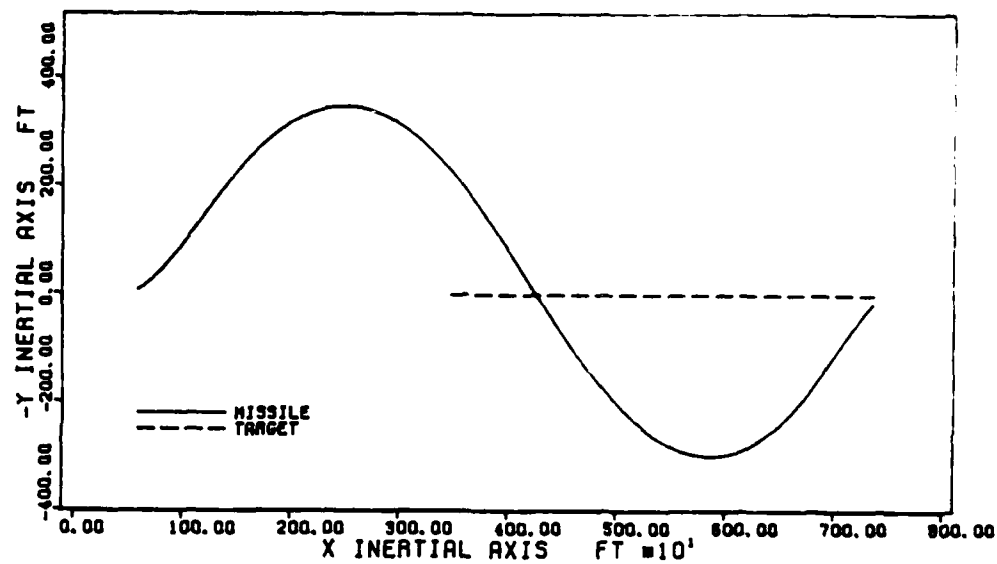


Figure 7. Best Information Horizontal Trajectory,
3000 Feet, 0 Degrees.

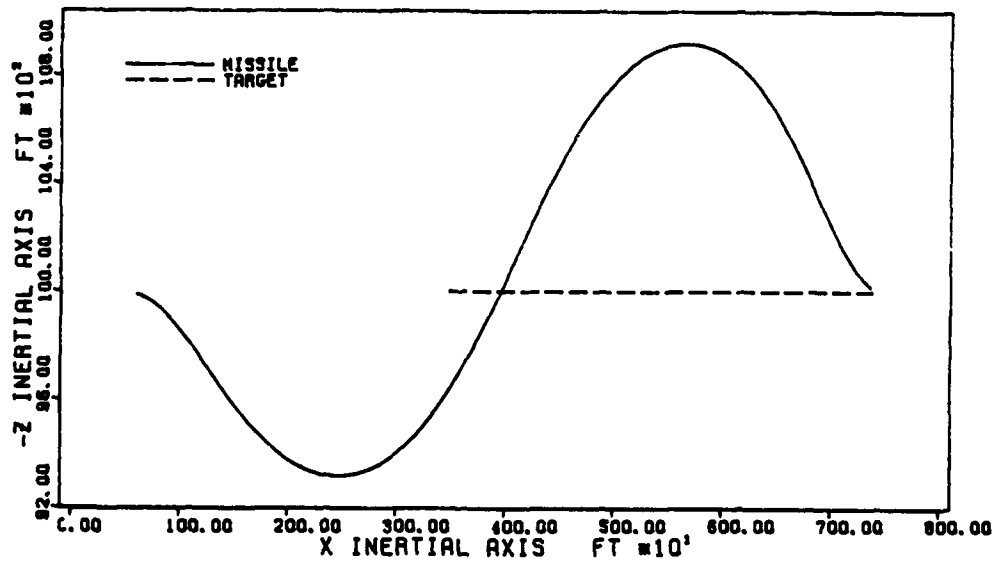


Figure 8. Best Information Vertical Trajectory,
3000 Feet, 0 Degrees.

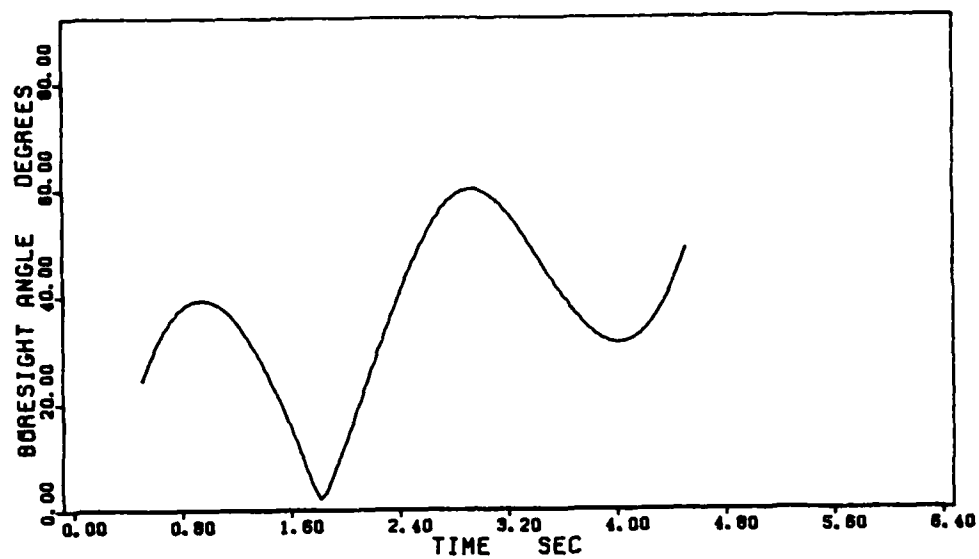


Figure 9. Best Information Boresight Angle,
3000 Feet, 0 Degrees.

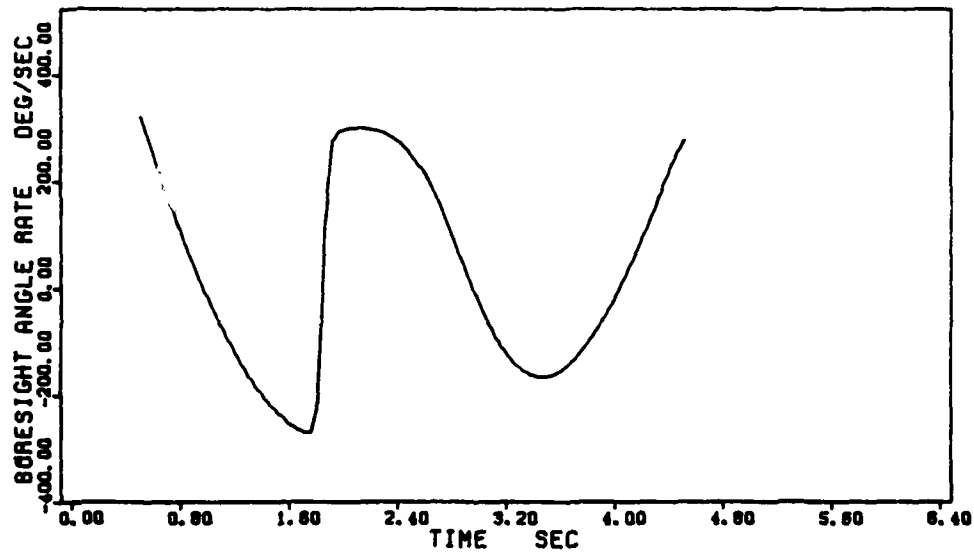


Figure 10. Best Information Boresight Angle Rate,
3000 Feet, 0 Degrees.

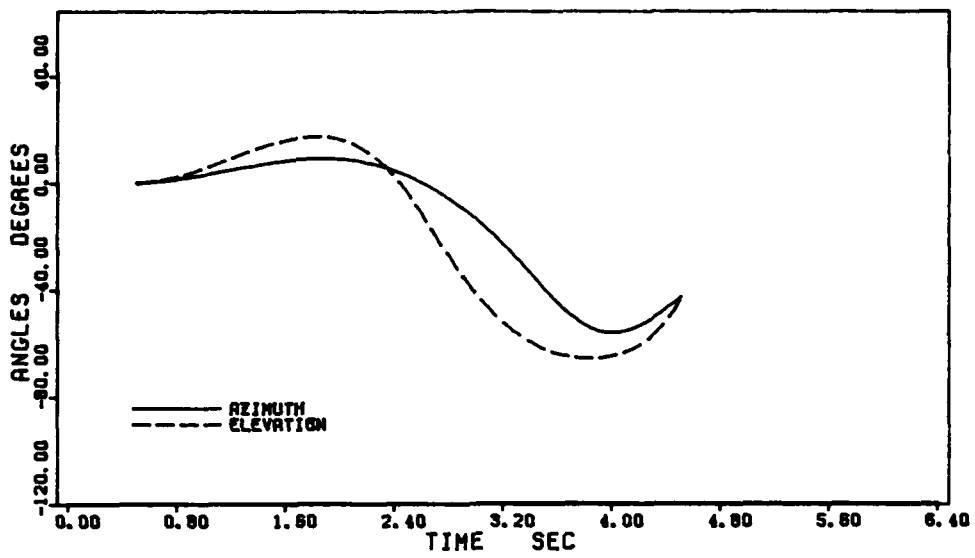


Figure 11. Best Information Az and El Angles,
3000 Feet, 0 Degrees.

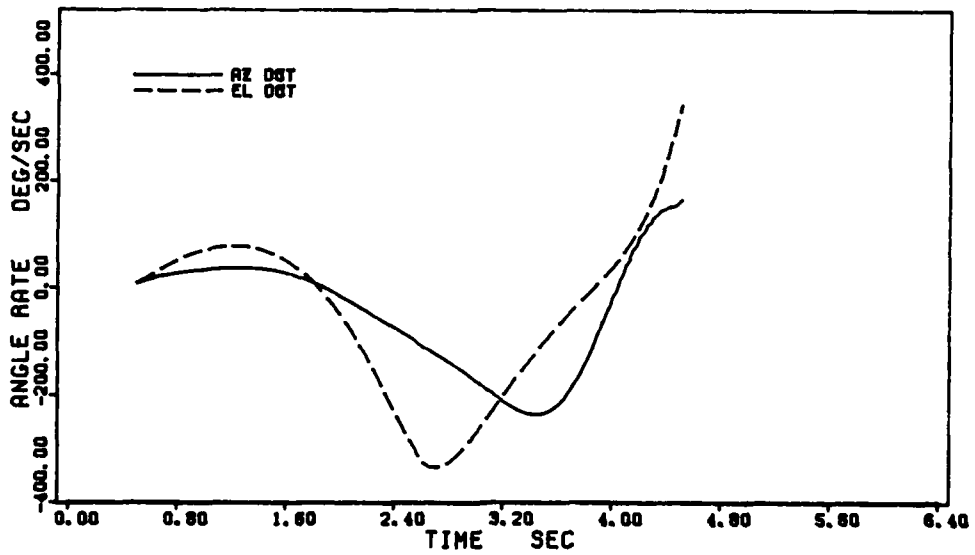


Figure 12. Best Information Az and El Angle Rates,
3000 Feet, 0 Degrees.

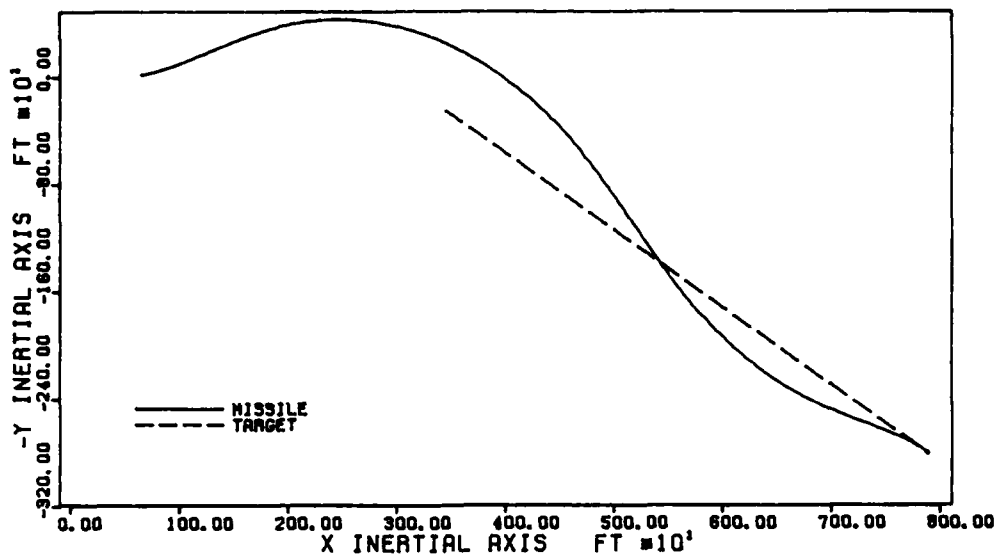


Figure 13. Best Information Horizontal Trajectory,
3000 Feet, 30 Degrees.

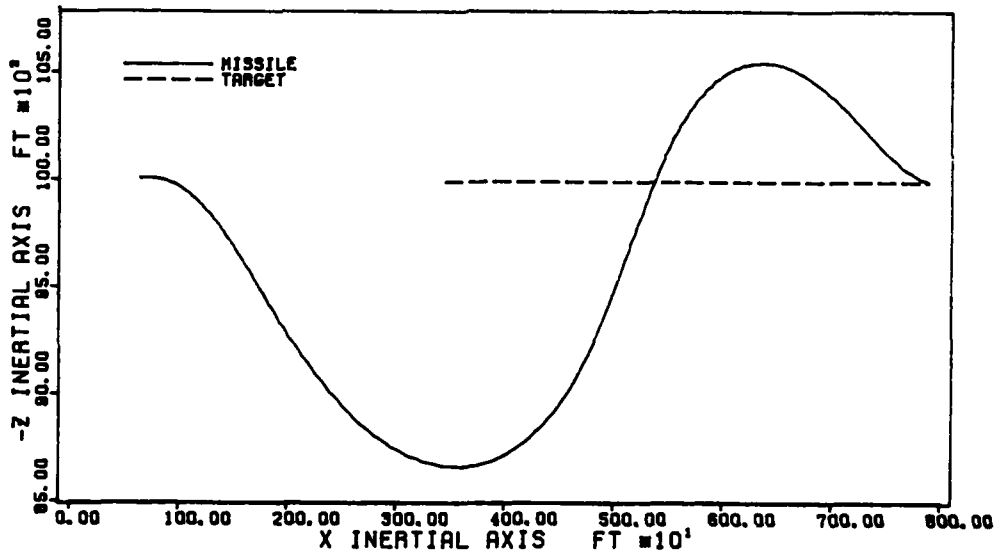


Figure 14. Best Information Vertical Trajectory,
3000 Feet, 30 Degrees.

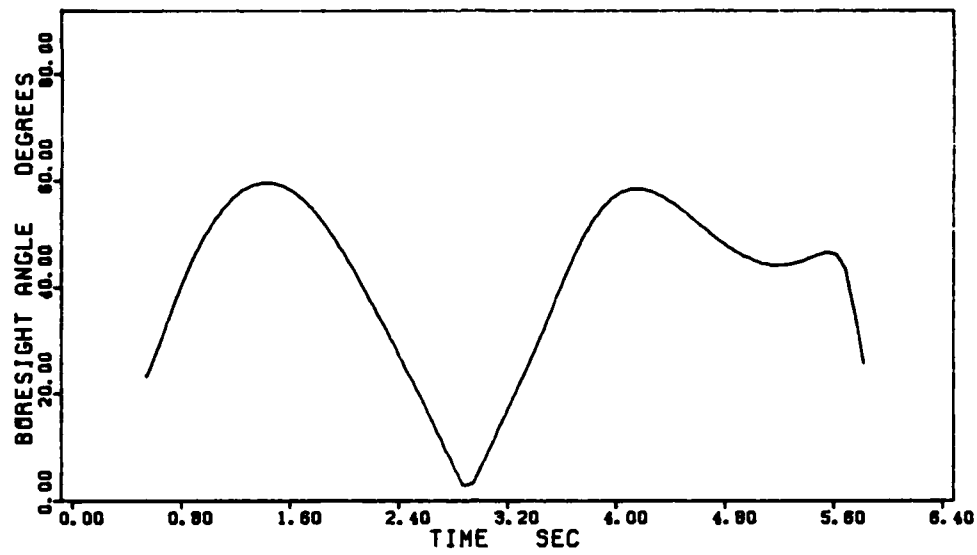


Figure 15. Best Information Boresight Angle,
3000 Feet, 30 Degrees.

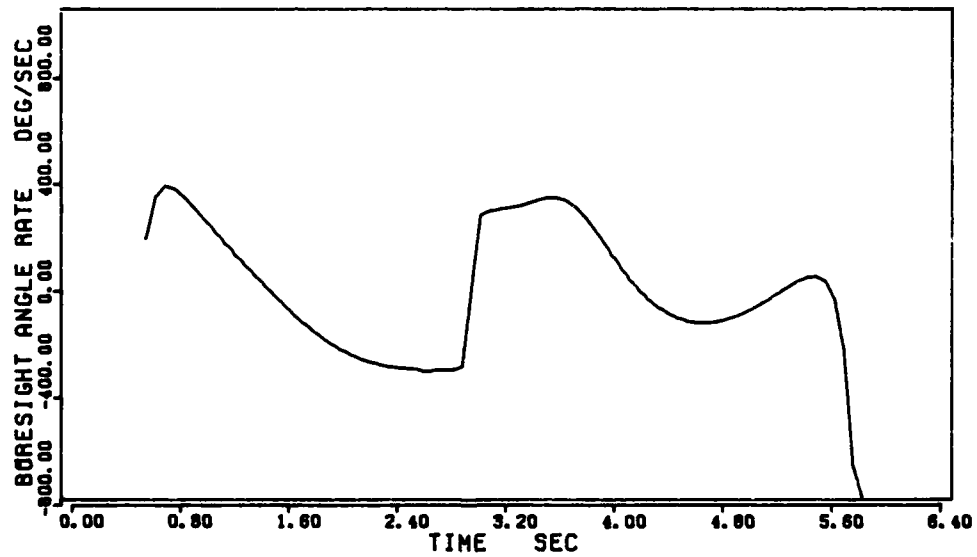


Figure 16. Best Information Boresight Angle Rate,
3000 Feet, 30 Degrees.

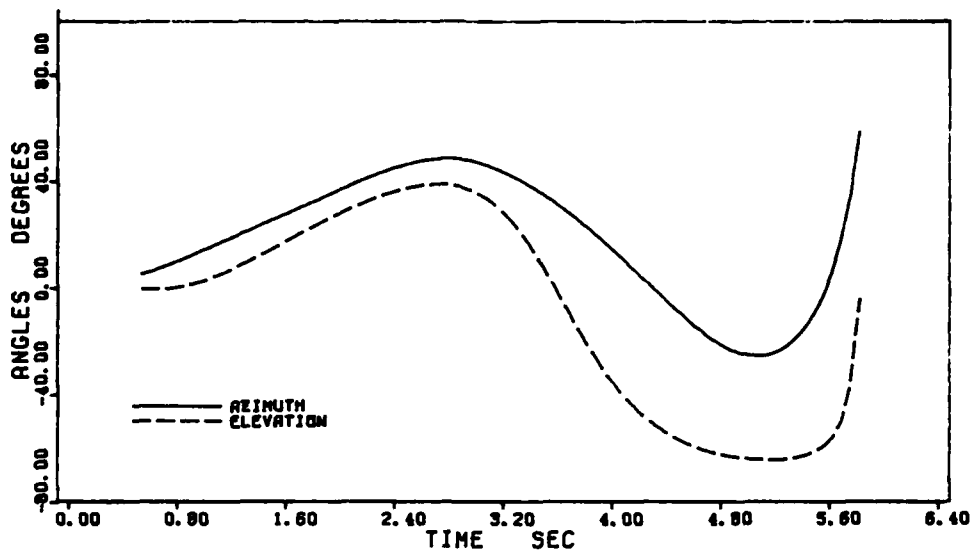


Figure 17. Best Information Az and El Angles,
3000 Feet, 30 Degrees.

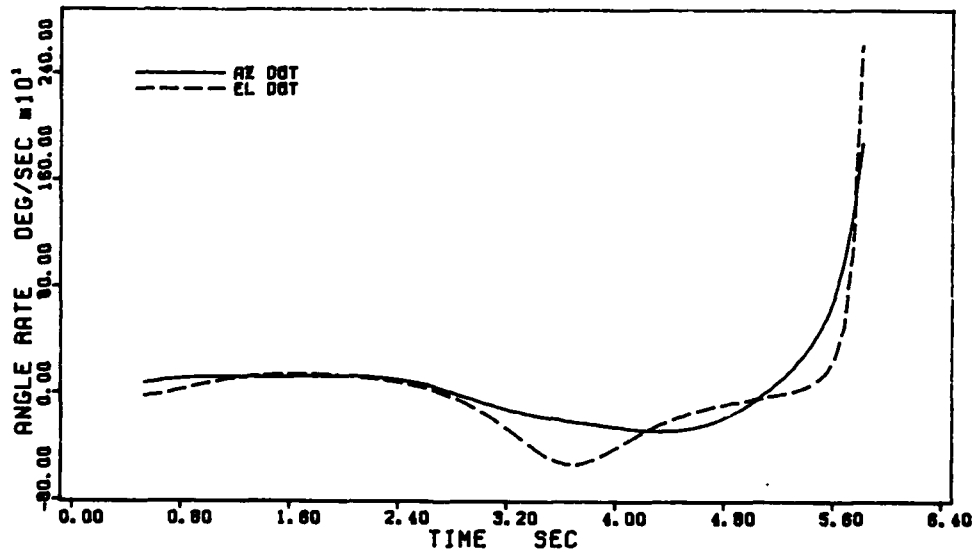


Figure 18. Best Information Az and El Angle Rates,
3000 Feet, 30 Degrees.

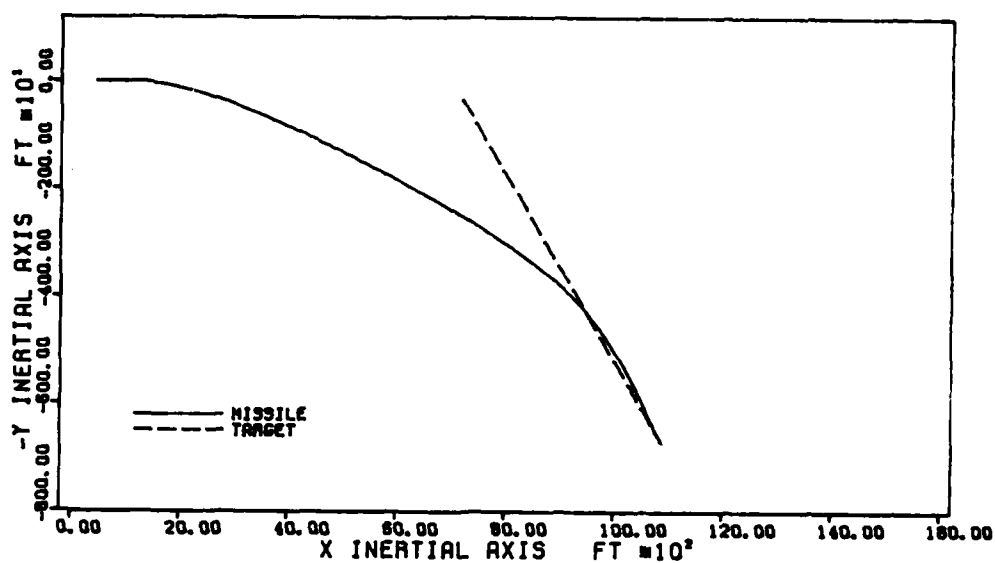


Figure 19. Best Information Horizontal Trajectory,
7000 Feet, 60 Degrees.

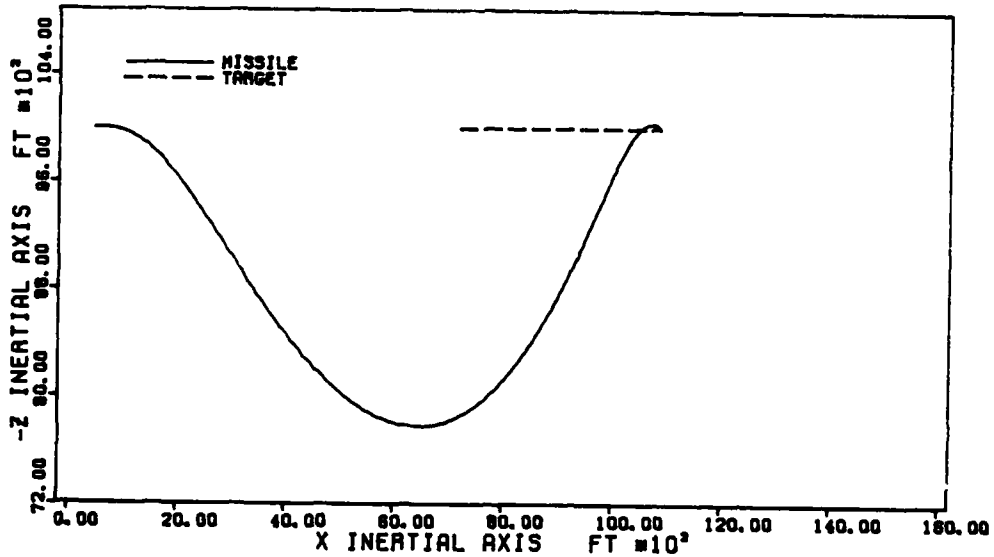


Figure 20. Best Information Vertical Trajectory,
7000 Feet, 60 Degrees.

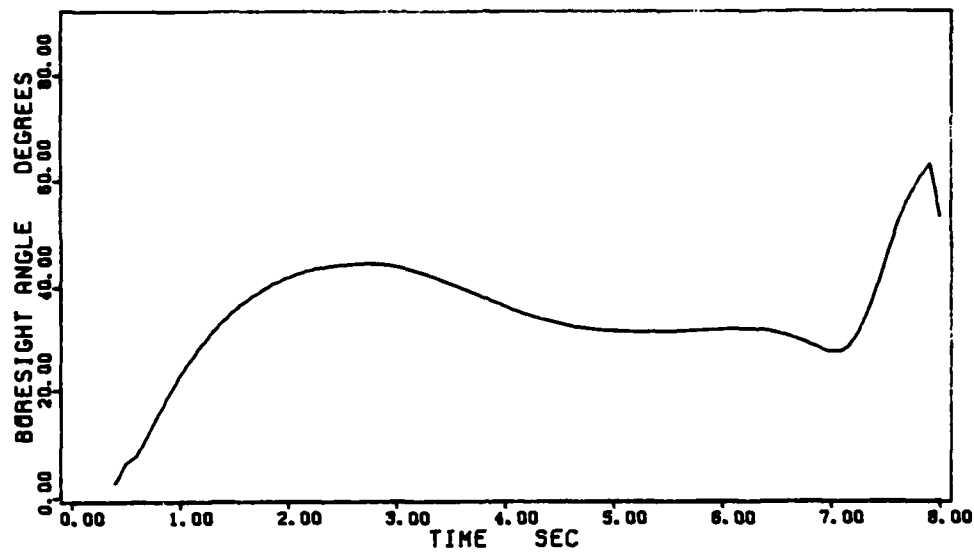


Figure 21. Best Information Boresight Angle,
7000 Feet, 60 Degrees.

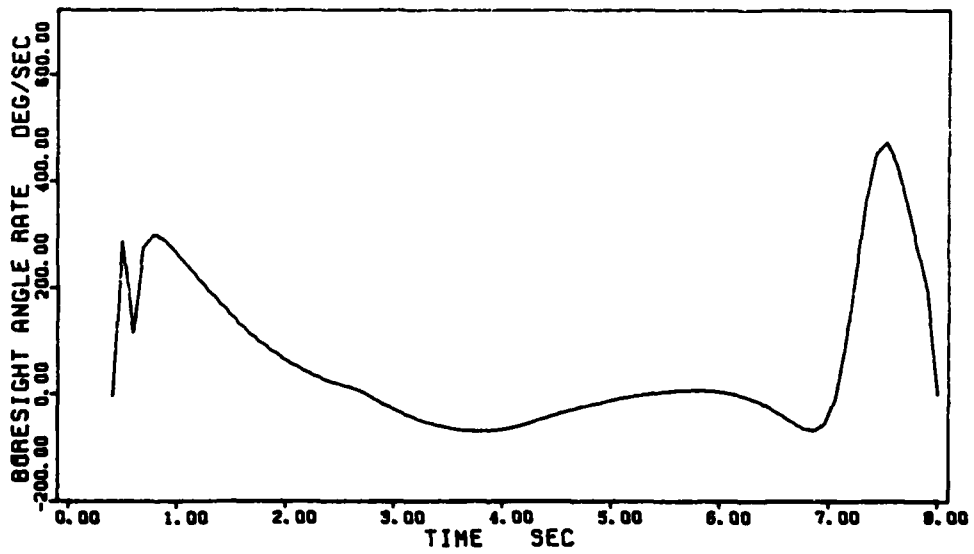


Figure 22. Best Information Boresight Angle Rate,
7000 Feet, 60 Degrees.

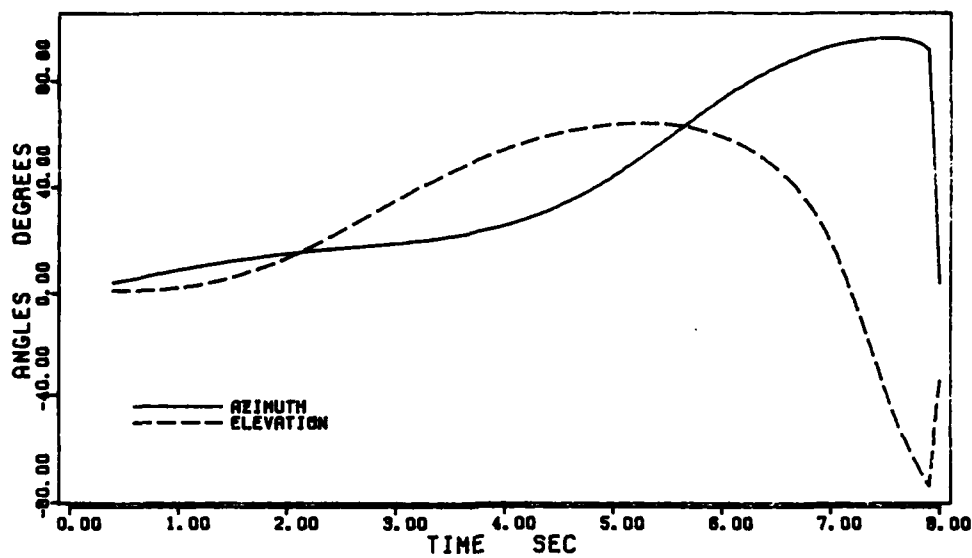


Figure 23. Best Information Az and El Angles,
7000 Feet, 60 Degrees.

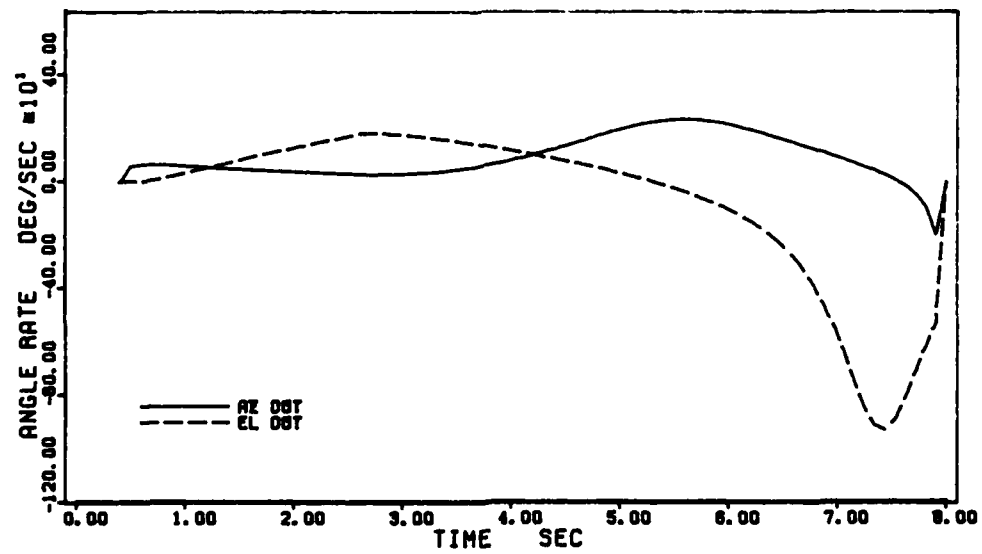


Figure 24. Best Information Az and El Angle Rates,
7000 Feet, 60 Degrees.

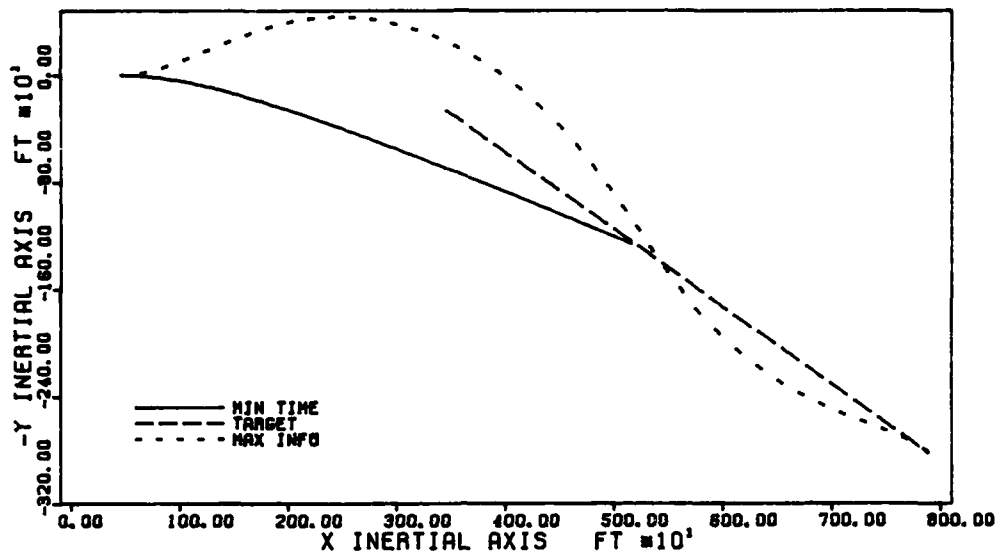


Figure 25. Minimum Time Horizontal Trajectory.

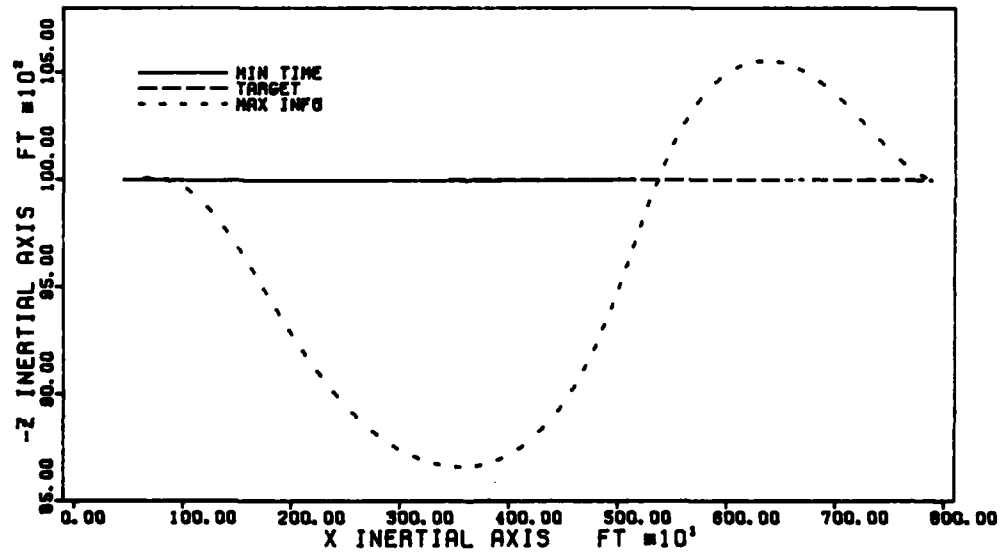


Figure 26. Minimum Time Vertical Trajectory.

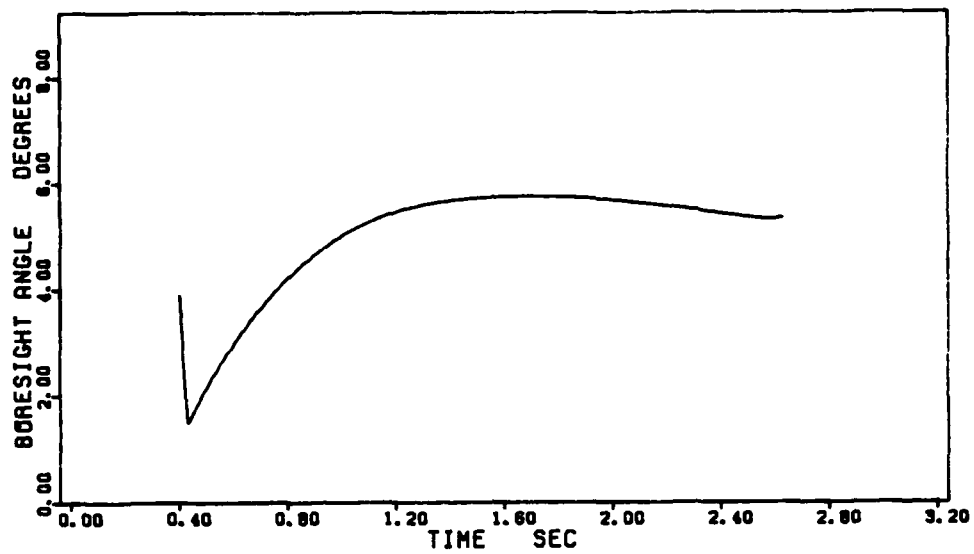


Figure 27. Minimum Time Boresight Angle.

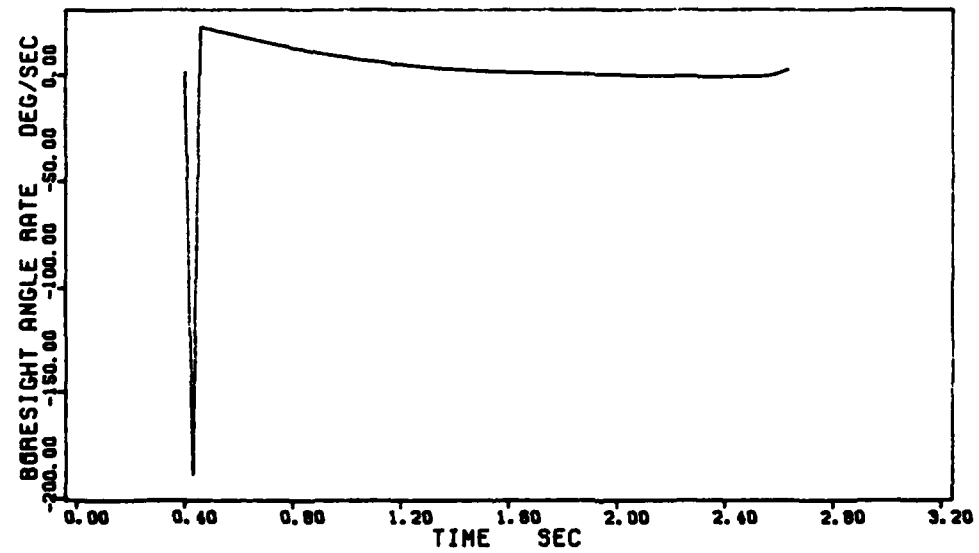


Figure 28. Minimum Time Boresight Angle Rate.

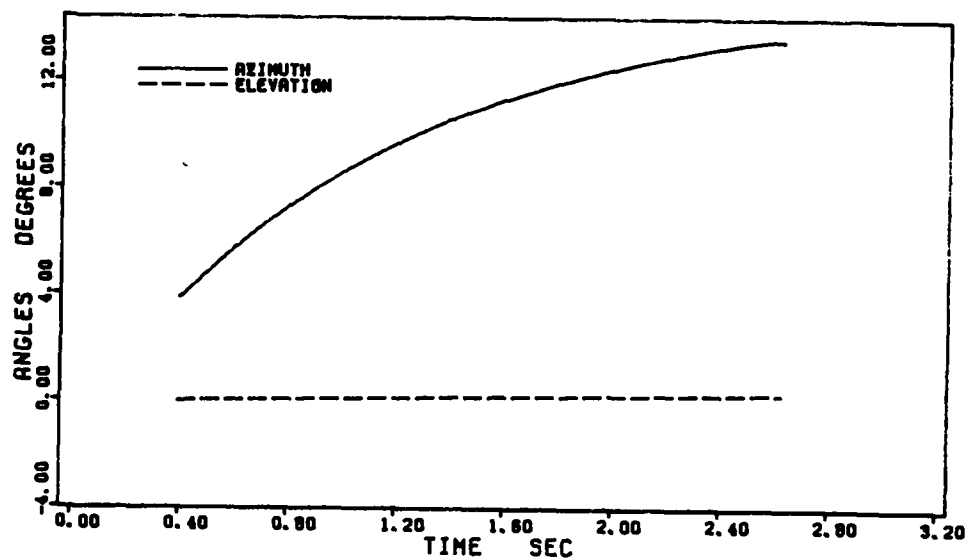


Figure 29. Minimum Time Az and El Angles.

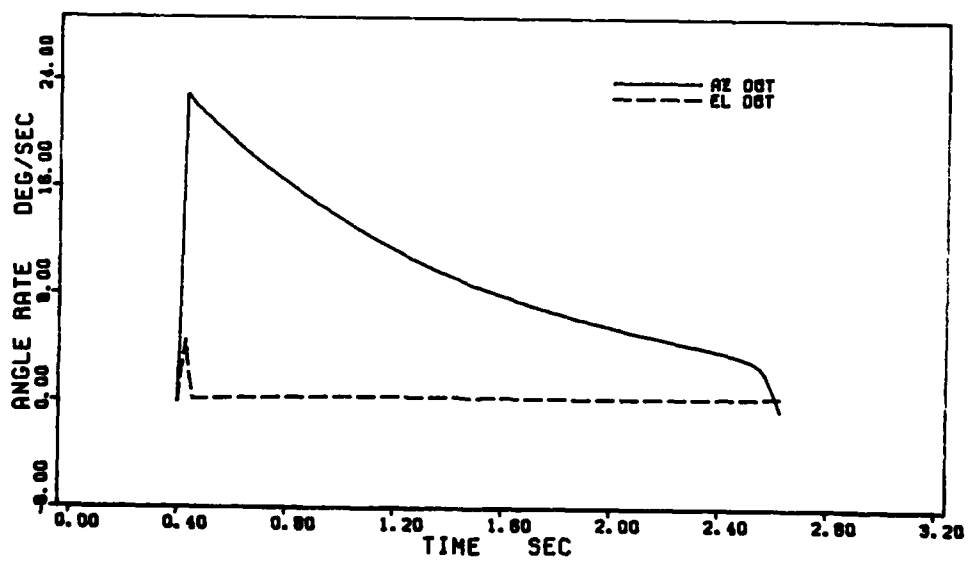


Figure 30. Minimum Time Az and El Angle Rates.

REFERENCES

1. Sammons, J.M., Balakrishnan, S., Speyer, J.L., and Hull, D.G., "Development and Comparison of Optimal Filters," U.S. Armament Laboratory, AFATL-TR-79-87, October, 1979.
2. Smith, R.C., "A Six-Degree of Freedom Computer Simulation of an Air-to-Air Missile Intercept," M.S. Thesis, The University of Texas at Austin, May, 1979.
3. Fletcher, R., "An Ideal Penalty Function for Constrained Optimization," J. Inst. Maths Applics. 15, 319-342, 1975.
4. Miele, A., Flight Mechanics, Theory of Flight Paths, Volume 1, Addison-Wesley Publishing Company, Inc., Reading, Massachusetts, 1962.
5. Jazwinski, A.H., Stochastic Processes and Filtering Theory, Academic Press, New York, New York, 1970.
6. Maybeck, P.S., Stochastic Models, Estimation and Control, Volume 1, Academic Press, New York, New York, 1979.

VITA

Stephen Wendell Larson was born in Ames, Iowa, on October 15, 1948, the son of Kenneth W. and Alice M. Larson. After graduation from Thomas Jefferson High School, Dallas, Texas, in 1966, he entered Purdue University. He received the degree of Bachelor of Science in Aerospace Engineering from the University of Texas at Arlington in May, 1971. He then entered Officer Training School and was commissioned in the United States Air Force in September, 1971. Following completion of Undergraduate Pilot Training in October, 1972, he was assigned as a T-33 pilot at Tyndall Air Force Base, Florida. In July, 1976, he was stationed at Langley Air Force Base, Virginia, as an F-106 pilot. He entered the Graduate School of the University of Texas in August, 1979, sponsored by the Air Force Institute of Technology.

Permanent Address: 3970 Cobblestone Circle
Dallas, Texas

This thesis was typed by Ann Jessen.

